Mon. Not. R. Astron. Soc. **000**, 000–000 (0000) Printed 5 February 2008 (MN LATEX style file v1.4)

Flat-spectrum symmetric objects with $\sim$ 1 kpc sizes I. The candidates

Pedro Augusto,[1] J. Ignacio Gonzalez-Serrano,[2] Ismael Perez-Fournon,[3] and Peter N. Wilkinson,[4]

[1] *Universidade da Madeira, Centro de Ciências Matemáticas, Caminho da Penteada, 9000-390 Funchal, Portugal*
[2] *Instituto de Física de Cantabria (CSIC-Universidad de Cantabria), 39005 Santander, Spain*
[3] *Instituto de Astrofísica de Canarias, c/ Via Láctea s/n, 38200 La Laguna, Tenerife, Spain*
[4] *University of Manchester, Jodrell Bank Observatory, Macclesfield, Cheshire SK11 9DL, UK*

5 February 2008

ABSTRACT

In order to understand the origin and evolution of radio galaxies, searches for the youngest such sources have been conducted. Compact-medium symmetric objects (CSO-MSOs) are thought to be the earliest stages of radio sources, with possible ages of $\lesssim 10^3$ yrs for CSOs (< 1 kpc in size) and 10^4–10^5 yrs for MSOs (1–15 kpc). From a literature selection in heterogeneous surveys, we have established a sample of 37 confirmed CSOs. In addition, we only found three confirmed flat-spectrum MSOs in the literature. The typical CSO resides on a $z \lesssim 0.5$ galaxy, has a flat radio spectrum ($\alpha_{thin} < 0.5$; $S_\nu \propto \nu^{-\alpha}$), is < 0.3 kpc in size, has an arm length ratio ≤ 2, and well-aligned ($\theta \leq 20°$) opposite lobes with a flux density ratio ≤ 10. In order to populate the 0.3–1 kpc size range (large CSOs) and also in order to find more flat-spectrum MSOs, we have built a sample of 157 radio sources with $\alpha_{1.40}^{4.85} < 0.5$ that were resolved with the VLA-A 8.4 GHz. As first results, we have 'rediscovered' nine of the known CSO/MSOs while identifying two new ~ 14 kpc MSOs and two candidate CSO/MSOs (which only lack redshifts for final classification). We were able to reject 61 of the remaining 144 objects from literature information alone. In the series of papers that starts with this one we plan to classify the remaining 83 CSO/MSO candidates (thanks to radio and optical observations) as well as characterize the physical properties of the (likely) many 0.3–15 kpc flat-spectrum CSO/MSOs to be found.

Key words: radio continuum: galaxies — galaxies: active — galaxies: evolution — galaxies: jets — galaxies: statistics.

1 INTRODUCTION

1.1 The evolution of extragalactic radio sources

The origin and evolution of extragalactic radio sources is one of the outstanding problems in Astronomy (e.g. de Vries et al. 1998a) and has been a fundamental problem in the study of active galaxies and their nuclei (AGN). These come in a variety of sizes, from compact (< 1 kpc) to very large (> 1 Mpc). This wide range of sizes has been interpreted as evidence for size evolution of the radio structure (e.g. Blandford & Rees 1974; Carvalho 1985; Fanti et al. 1995; Readhead et al. 1996a,b). In the standard model of AGN, a central supermassive black hole, with $\sim 10^6$–10^9 $M_\odot$ feeds on the material of the host galaxy to produce two opposing radio emitting jets, thus creating a symmetric source that might only be disturbed by the environment/speed of the jets, unless its source runs out of fuel. Mature radio galaxies fit into this picture and are mostly split up into Fanaroff & Riley (1974) type I and type II radio galaxies (FRI and FRII). Up to 10^5 times smaller, compact-medium symmetric objects (CSO-MSO) might be their precursors (e.g. Readhead et al. 1996a,b).

Traditionally, CSO/MSOs have always been considered high-power radio sources. However, low-power sources must be considered as well, if we really want to tell a story about the evolution of small (and young) radio sources all the way until becoming large radio galaxies (FRII *or* FRI) — e.g. Marecki et al. (2003). Fanti et al. (1995) already pointed out the hypothesis of MSOs evolving not into FRIIs but into FRIs and despite their bias towards high-power CSSs they concluded that, really, only the most powerful MSOs could be the precursors of FRIIs. Similar conclusions were reached by Readhead et al. (1996b), while Middelberg et al. (2004) go as far as proposing the radio structure of NGC7674 (a

Seyfert galaxy) as the one of a (very weak) CSO. Begelman (1996) considered both hypothesis: lower power CSO/MSOs would evolve into FRIs while the high power ones would become FRIIs. In order to constrain models it is important to extend the radio power range (Fanti et al. 2001).

For example, the square-root decrease with size of the luminosity from CSOs to FRIIs proposed by Begelman (1996) and Fanti et al. (1995), using the border value of 1×10^{25} W/Hz*, implies that a ~ 1 Mpc FRII evolved from a 10 pc CSO with a $> 3 \times 10^{27}$ W/Hz power, through a 10 kpc MSO with $> 1 \times 10^{26}$ W/Hz. This is why the total radio power of CSO/MSOs was assumed to be $\sim 10^{26}$–$10^{27} h^{-2}$ W/Hz in earlier surveys (e.g. Phillips & Mutel 1982; Readhead et al. 1996a; Fanti et al. 1995; Murgia et al. 1999). Recent surveys (e.g. Kunert-Bajraszewska et al. 2005) include much weaker sources.

'Hot-spots' in CSOs are so close (<1 kpc) to the nucleus that they might help towards the understanding of the central engines in AGN (Readhead et al. 1996a,b). Furthermore, they are unique probes to the physics of the gas clouds of the broad line-emitting region — Readhead et al. (1996a). MSOs, being larger (1–15 kpc), are ideal to probe the ISM further away from the nucleus (including the clouds in the narrow line-emitting region (NLR) and extended NLR). They might also be the middle link for the hypothetical evolution of CSOs into FRIIs or FRIs.

Assuming the jet to travel at the speed of light we get upper limits of 10^{3-4} years for $\sim$ 1 kpc CSO/MSOs (large CSOs and small MSOs). Furthermore, kinematic measurements on ten CSOs (Giroletti et al. 2003; Ojha et al. 2004; e.g. Polatidis & Conway 2003) give $v \simeq 0.05$–$0.3 h^{-1}$ c (hotspot advance speed) which, assuming constant speeds since source ignition (e.g. Readhead et al. 1996b), give ages of ∼300–2000 yrs. These are consistent with sychrotron loss time scales ($\sim$ 1200–5000 yrs; e.g. Readhead et al. 1996a; Giroletti et al. 2003). CSOs evolve fast (c.f. FRIIs lobe advance speed ~ 0.06 c), explaining their 'rarity': only ∼10% of radio sources with compact structure are CSOs (Readhead et al. 1996a), getting down to 1% for the flat-spectrum ($\alpha_{1.40}^{4.85} < 0.5$) largest CSOs and small MSOs (Augusto et al. 1998).

There are still two possibilities for the origin of CSO/MSOs, summarized in what follows.

Youth scenario: The most popular view is that in which CSOs evolve into MSO/Compact Steep Spectrum Sources† (CSSs; $\alpha_{thin} > 0.5$ with $S_\nu \propto \nu^{-\alpha}$) which, in turn, evolve into FRIIs — e.g. Phillips & Mutel (1982); Carvalho (1985); Begelman (1996); Readhead et al. (1996b); Kunert et al. (2002); Perucho & Martí (2002). The intermediate ~ 1 kpc stage should be a CSS in the case of self-similar expansion (lobes expand with growth) or a flat-spectrum MSO in case the expansion is non-self-similar (hot spots remain compact, if seen at all). Maybe less luminous CSOs evolve into FRIs via a Giga-Hertz Peaked Spectrum Source (GPS) stage (O'Dea 1998; de Vries et al. 1998b).

Re-born scenario: From an analytical model of the evolution of double radio sources < 100 kpc, Alexander (2000) extended Kaiser & Alexander (1997) model to $\sim$ kpc scales: a population of 'short-lived' sources is predicted, where the jets are disrupted before reaching the $\sim$ 1 kpc core radius (King density profile) of the host galaxy. This could be interpreted in the context of "re-birth". For example, Baum et al. (1990) show the 47 pc CSO B0108+388 to have weak radio emission on tens of kpc scales; this might be an unrelated source or evidence for recurrent activity.

1.2 Definitions

Over the last twenty years, a panoply of names have been used to classify < 15 kpc-sized sources which might be the precursors of the much larger FRI/FRII radio galaxies. Usually applied in the 'young radio source' context, we have CSOs, MSOs, CSSs, GPSs, and, the oldest of all, compact doubles (CDs). It is still disputed whether CSOs are included in the GPS class (e.g. Snellen et al. 1999, O'Dea 1998, Marecki et al. 1999 *vs.* Stanghellini et al. 1997a, Stanghellini et al. 1999, Fassnacht & Taylor 2001). In Figure 1 we summarize the current (confused) status and in Table 1 we propose a 'non-grey zone' radio classification for all these sources, which can be used for the time being, at least operationally: since CSO/MSOs are a more homogenous class than GPSs are (Fassnacht & Taylor 2001), we propose to split up the two main sets of 'young sources' into the ones selected by morphology (CSO/MSOs) and the ones selected spectrally (CSS/GPSs). For CSO/MSOs, in particular, it should be made clear that it is not necessarily true that an edge brighened lobe is an hotspot. It might just be a knot in a longer jet. However, the likelihood that we get two of those opposed to each other and they are not hotspots is small. It is on this basis that CSO/MSOs with only two components are confirmed. When we come to triple (and more) component sources the hotspot/edge-brightened lobe definition relaxes: if we identify a central core component then we have a CSO/MSO structure (even if no obvious hotspots or edge-brightening is seen in any terminal lobe).

Historically there has been a bias against steep-spectrum CSOs and flat-spectrum MSOs (e.g. the "CSO-finding" $\alpha < 0.5$ Caltech-Jodrell Bank surveys (e.g. Wilkinson et al. 1994); the "CSS ($\supset$MSO) finding" $\alpha > 0.5$ Bologna-Jodrell-Dwingeloo survey — e.g. Fanti et al. 1995).

1.2.1 CDs

Compact double (CD) is the name from where all names come from: CSO/MSO/CSS/GPS. In fact, the classification CD remains, for example, when no core is seen in a candidate CSO/MSO. Phillips & Mutel (1982) and Carvalho (1985) "compact symmetric (double) sources" were defined with no

* The formal boundary from Fanaroff & Riley (1974) is at 178 MHz: 5.3×10^{25} W/Hz with our cosmology. A typical radio galaxy ($\alpha_{0.178}^{1.4} = 0.8$) has $L_{1.4} = 1 \times 10^{25}$ W/Hz while a flat spectrum CSO/MSO ($\alpha_{0.178}^{1.4} = 0.4$–$0.5$) has $L_{1.4} = 2 \times 10^{25}$ W/Hz.

† The original definition is on Peacock & Wall (1982), with $\alpha_{2.7}^{5} \geq 0.5$ (now as far as $\alpha_{0.325}^{1.4}$ — e.g. Tschager et al. 2003), who also define almost half of their sample as "compact" and with "steep" spectra; in an historical perspective, up to this time *compact* $\Leftrightarrow$ *flat spectrum* and *extended* $\Leftrightarrow$ *steep spectrum*. Phillips & Mutel (1982) demand an optically thin regime with $\alpha_{\nu_1}^{\nu_2} \geq 0.5, \nu_1, \nu_2 > 1$ GHz. We define α_{thin} from a full spectrum linear fit to the part that is optically thin for frequencies greater than a given peak; if there is no peak, it is inferred to lie at some still unobserved low frequency and the full spectrum is used.

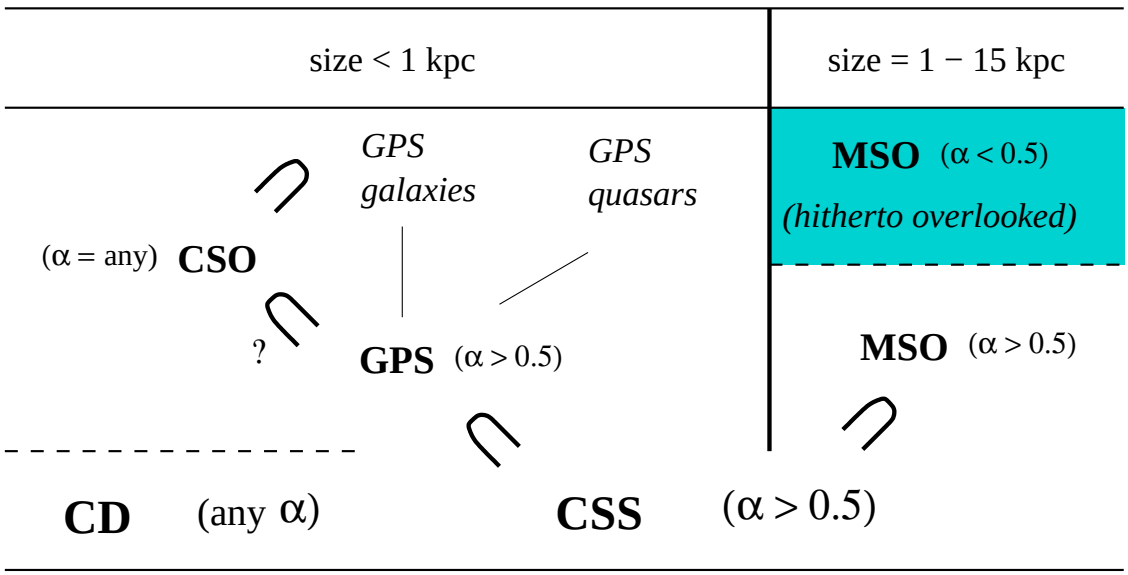

Figure 1. The currently messy (and incomplete) situation in the definition of CSOs, MSOs, CSSs, GPSs and CDs. CDs and CSSs cover all ranges of sizes. The latter includes GPSs and MSOs, the first generally < 1 kpc and the latter showing symmetric structure straddling a (putative or not) central nucleus. CSOs also appear with flat-spectrum ($\alpha < 0.5$) and, in this sense, they cannot be paralleled to GPSs (even if only the ones identified with galaxies); in any case, there is no evidence for complete overlap of GPSs and CSOs. MSOs with a flat-spectrum (upper right corner) have been overlooked.

Table 1. Our proposed dual-view radio classification for CSOs, MSOs, CSSs and GPSs. CDs fall out of this picture since they can be all or none (when one-sided core-jet sources). The scheme below must be viewed as operational only, since in the coming years more knowledge of the sources involved might suggest a different one. Note that we give strict morphological criteria to confirm the classification of CSO/MSOs; also that the latter are similar, apart from size (MSOs can be flat-spectrum radio sources).

Classification		*Two components (lobes)*	*Three/more components*
morphological	CSO (<1 kpc) MSO (1–15 kpc)	edge-brightness clearly seen in *both* or kinematics show opposed motion	(one of the) central component(s) proved as the core
		Spectral turnover	*GPS/CSS classification references*
spectral ($\alpha_{thin} > 0.5$)	GPS (<1 kpc)	0.5–10 GHz	Fanti et al. (1995) de Vries et al. (1997)
	CSS (<15 kpc)	$\lesssim$0.1–0.5 GHz	O'Dea (1998) Tschager et al. (2003)

central core and a ratio of flux density between the two lobes $\leq$1.5, $\alpha_{thin} \geq 0.5$ (except 3C394 with 0.4), sizes <0.1 kpc, ages 10^3–10^4 yrs, and $v \simeq 0.2$ c (theoretical lobe advance speed).

1.2.2 CSOs (< 1 kpc)

A CSO (Wilkinson et al. 1994; Conway et al. 1994) is a compact radio source with two outer edge-brightened lobes/hotspots or twin-jets plus a (possibly putative) central core. Symmetry is essential so, operationally, the arm ratio should be ≤ 10, although the flux density ratio (between lobes) is not constrained (it is frequency-dependent). CSOs have weak polarization and variability (< 10% in a few years): some are so stable that they might be excellent VLBI flux density calibrators — Fassnacht & Taylor (2001).

1.2.3 CSSs (<15 kpc)

This class of source, with a subgalactic size and a steep spectrum ($\alpha_{thin} > 0.5$), has more pronounced lobe flux density ratios and/or arm ratios than CSOs (Fanti et al. 1990; Fanti et al. 1995; Dallacasa et al. 1995; Sanghera et al. 1995; O'Dea 1998). When with a spectrum peak at $\nu > 0.5$ GHz they are classified as GPSs (Section 1.2.4) while when symmetric (most — e.g. Readhead et al. 1996a; Fanti et al. 1995; Kunert-Bajraszewska et al. 2005) they are called MSOs (Section 1.2.5). They show low radio polarizations and little vari-

ability although up to an order of magnitude more variable than the most stable CSOs (Fassnacht & Taylor 2001).

1.2.4 GPSs (< 1 kpc)

In most properties, GPSs are similar to CSSs. The main difference is in the spectral peak (c.f. Table 1; e.g. Tornikoski et al. 2001): the canonical turnover frequency of GPSs is 1 GHz — de Vries et al. (1997). Also, many are highly variable (mostly identified with quasars — Torniainen et al. 2005) jeopardizing their usual classification when based only on sparse spectral data points (both in observing epochs and in frequency) — Stanghellini et al. (1998) and Tornikoski et al. (2001).

1.2.5 MSOs (1–15 kpc)

So far regarded as steep-spectrum sources, we here point out the existence of $\alpha < 0.5$ flat-spectrum MSOs (c.f. Sections 2.3 and 4) as a hitherto not considered type of source (they fill the "empty corner" in Figure 1). Augusto et al. (1998) mention many candidates for such sources. Flat-spectrum MSOs could be the sources into which CSOs evolve when the expansion is non-self-similar (de Young 1997; Tschager et al. 2000). The statistics of MSOs are relevant in order to inspect which evolutionary scenario (non-self-similar vs. self-similar expansion) dominates.

1.3 The optical hosts

Not much is known at optical wavelengths about CSOs since only a few cases have been studied (Taylor et al. 1997). Readhead et al. (1996a) and Bondi et al. (1998) found that the hosts of five CSOs are mostly $m_V \sim 20$–22 elliptical galaxies (0.3–1 L^*) with strong narrow emission lines; the continuum is characteristic of an old stellar population. Detailed HST views of three nearby ($z \lesssim 0.1$) CSOs (Perlman et al. 2001) confirm residence in normal ellipticals but with ten times more dust than radio elliptical galaxies.

A lot more is known in the optical about CSS/GPSs, which have similar redshift distributions and have as hosts $0.1 \lesssim z \lesssim 1$ regular giant elliptical galaxies (many interacting), like FRIIs do, a fact consistent with a GPS → CSS → FRII source evolution (O'Dea 1998; de Vries et al. 2000). GPS galaxies ($z \sim 0.3$) show a CSO morphology while the quasars ($z \sim 2$) do not (O'Dea et al. 1991; de Vries et al. 1998b; Snellen et al. 1999; Stanghellini et al. 2001).

1.4 This paper

The total number of confirmed CSOs is relatively small (37 — Section 2; 25 have linear size information) for a two orders of magnitude size range (0.01–1 kpc). Worse, only three $\alpha < 0.5$ flat-spectrum MSOs (1–15 kpc) and four 'large CSOs' (0.3–1 kpc) are confirmed, so far. The lack of 'large CSOs' and flat-spectrum MSOs might be explained by a CSO 'preferred' evolution into CSSs (e.g. Section 1.1; Augusto et al. 1998), but we need better statistics.

The aim of the series of papers which starts with this one is to find a fairly large number of $\alpha_{1.40}^{4.85} < 0.5$ flat-spectrum CSO/MSOs with ∼kpc sizes (large CSOs and MSOs). We start by establishing the current sample of confirmed CSOs as well as describing their overall properties (Section 2). In Section 3 we build up a 157-source sample out of which we expect a few tens to be confirmed as CSO/MSOs when our study is complete. We conclude with a brief summary (Section 4).

Throughout the paper we use an $\Omega_m = 0.3$, $\Omega_\Lambda = 0.7$, $H_0 = 75$ km/s/Mpc cosmology.

2 CONFIRMED SYMMETRIC SOURCES

The literature abounds with examples of confirmed CSOs (summarized in Section 2.1) while MSOs are only abundant as CSSs, i.e., with a steep spectrum. Flat-spectrum MSOs are rare (Section 2.3).

2.1 The sample of CSOs

In Table 2 we present all currently known confirmed CSOs, proved as such from maps (or kinematics, in a few cases) in our extensive literature search. We were very rigorous in our classification, using the criteria of Table 1. All relevant maps/information have been compiled and carefully scrutinized before listing a given CSO as "confirmed" beyond any reasonable doubt. Everytime the candidate had three or more components (even when some doubt remains about which of the central components really is the core), we required a confirmed central core usually from, at least, two-frequency data. If having only two components, they must be edge-brightened lobes: assumed is a putative central core (c.f. Taylor et al. 1996a; Taylor & Vermeulen 1997; Bondi et al. 1998; Polatidis et al. 1999). 'Hotspots' are not necessarily required for sources with three (or more) components; all we need is emission on both sides of the core (even if jet-like). This is the usual way CSOs have been identified (see, for example, Readhead et al. 1996a; Stanghellini et al. 1997a; Peck & Taylor 2000). Since CSOs have sizes < 1 kpc, we rejected all sources with size > 1 kpc and since, by definition, they are symmetric sources (e.g. Readhead et al. 1996a,b), we ruled out any with an arm ratio $R > 10$. Figure 2 defines and explains the calculation of the radio map parameters in Columns (10) and (13)–(16) of Table 2.

In five CSOs studied, Taylor et al. (1996a) find considerable flux density ratio asymmetries in the two opposing jets, possibly due to differences in density of the surrounding medium (Stanghellini et al. 1997a). Furthermore, flux density ratios depend on frequency. Hence, it seems more dangerous to place a limit on such ratio and we do not do it. We also do not constrain arm angles (column (16) of Table 2) since, for example, we have $\phi = 148^\circ$ (misalignment θ is 32°) for a 'classic' CSO (B2021+614) and only three CSOs in the Table are more misaligned (reaching a minimum of $\phi = 134^\circ$ for B1543+005, a Peck & Taylor (2000) CSO).

Comments on the sources marked with * in Column (1) of Table 2 follow: **B0046+316:** This is a Sy2 galaxy; it possibly has a core-jet radio structure in a weird geometry (Anton et al. 2002). **B0424+414, B0500+019, B0646+600, B0703+468, B0710+439:** These sources are also classified as GPSs (e.g. O'Dea et al. 1991; Marecki et al. 1999; Stanghellini et al. 2001). **B1934-638:** This is the archetype GPS (e.g. Tzioumis et al. 1989).

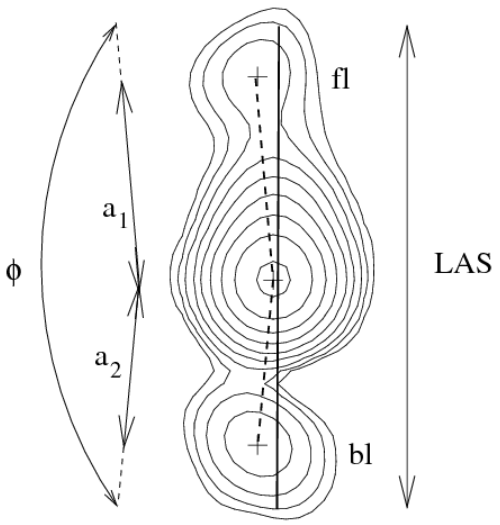

Figure 2. In order to help understanding the parameters measured for each source in Columns (10) and (13)–(16) of Table 2, we here present a case with an actually located core (without which, only Columns (10), (13) and (14) might have values). Most maps in the literature are presented, like this one, with the lowest contour at three times the r.m.s. noise on the map (3σ). Then, in order to estimate its angular size (LAS), we measure the largest possible extent on the 6σ contour. Next, we locate the core and each lobe peak (marked with crosses) and immeditately identify the strongest lobe (*bl*) from the contours alone, deriving a peak flux density estimate. The same is made for the faintest lobe (*fl*) and the nucleus, whereby calculating the values in Columns (13) and (14). Finally, joining by segments the crosses that correspond to the two lobes and the nucleus, we estimate ϕ (Column (16)) and $R = \frac{a_1}{a_2}, a_1 > a_2$ (Column (15)).

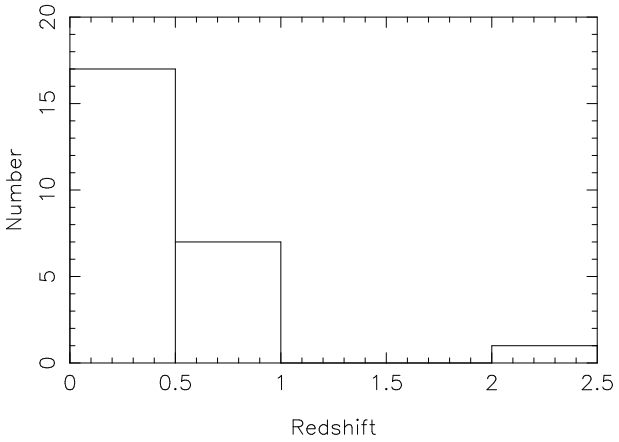

Figure 3. The redshift distribution of 25 CSOs, with 68% completeness.

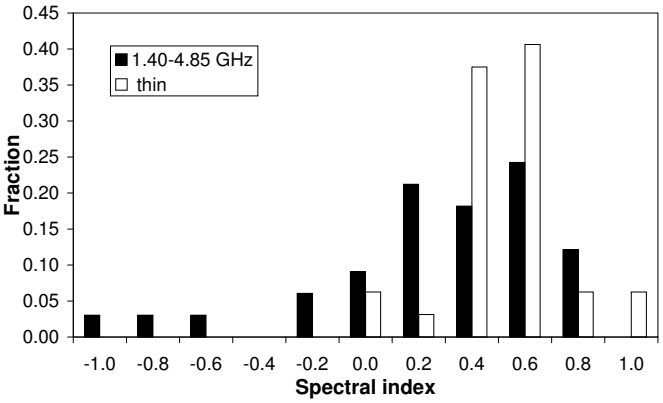

Figure 4. The compared spectral indices ($\alpha_{1.40}^{4.85}/\alpha_{thin}$ — see Table 2) distributions of 33/32 CSOs, with 89%/86% completeness.

2.2 Statistics

Since all confirmed and candidate CSOs of Table 2 have been extracted from different samples in the literature with no other selection criteria except for morphology, the statistical results must be taken with caution since they might not be representative of the CSO class. We list 41 sources in Table 2 out of which four (labelled "CSO?") still might be MSOs if their sizes turn out to be 1–15 kpc: we keep them in the table until we have enough data to finally classify them. This leaves us with 37 certain CSOs which we use in the statistical study that follows.

The optical information on the 27 CSOs that do have it (73% completeness) shows that galaxies are clearly the typical host (23 or 85%) while only four sources (15%), at most, reside in quasars. In Figure 3 we present the redshift distribution of the sample (25 sources; 68% complete). We clearly see a concentration towards low redshifts, with 17 (68%) sources at $z < 0.5$, implying a nearby galactic host population. In fact, except for one quasar, all CSOs reside in $z < 1$ hosts. The 25 CSO median is[‡] $z_{25} = 0.36^{+0.16}_{-0.14}$. The quasar statistics (only three: they do not change the median at all) are still too poor to conclude that, like for GPSs, the hosts/redshifts imply two independent populations.

As regards to spectral indices, since we use a flat-spectrum sample defined from $\alpha_{1.40}^{4.85} < 0.5$ (Section 3), we included this quantity for all CSOs in Table 2, in addition to α_{thin}. Usually, to select CSOs or CSSs from weak samples, only a two frequency spectral index is used/available — see e.g. Kunert et al. (2002). Figure 4 shows the $\alpha_{1.40}^{4.85}/\alpha_{thin}$ distribution for 33/32 of the 37 CSOs of Table 2 (89%/86% complete). Although CSOs, by definition, have no spectral restrictions, it turns out that the majority have a flat radio spectrum (23, or 70% with $\alpha_{1.40}^{4.85} \leq 0.5$; 18, or 56% with $\alpha_{thin} \leq 0.5$). The medians are $\alpha_{1.40\ (33)}^{4.85} = 0.3^{+0.2}_{-0.1}$ and $\alpha_{thin\ (32)} = 0.5 \pm 0.1$. There is a tendency for $\alpha_{1.40}^{4.85}$ being flatter than α_{thin}. In fact, defining $\Delta\alpha = \alpha_{1.40}^{4.85} - \alpha_{thin}$, we have $\Delta\alpha_{29} = -0.1 \pm 0.1$ (only 29 CSOs have both $\alpha_{1.40}^{4.85}$ and α_{thin} values available).

[‡] The subscripts in the medians show the actual number of sources with values available for each calculation. We give the asymmetric error of the median at the 95% confidence level.

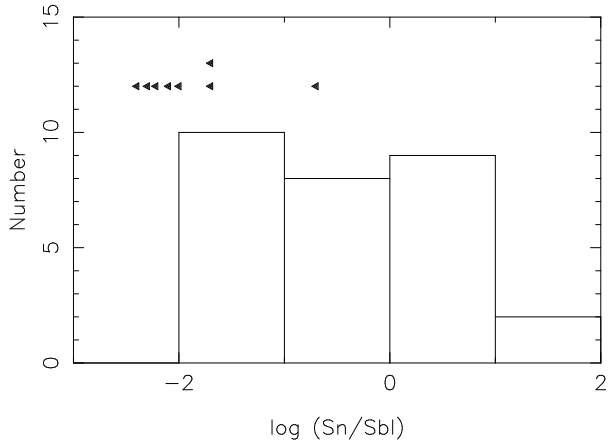

Figure 5. The flux density ratio (nucleus over bright-lobe) distribution for 29 CSOs — 78% complete (the eight cases where no core is located are included as upper limits).

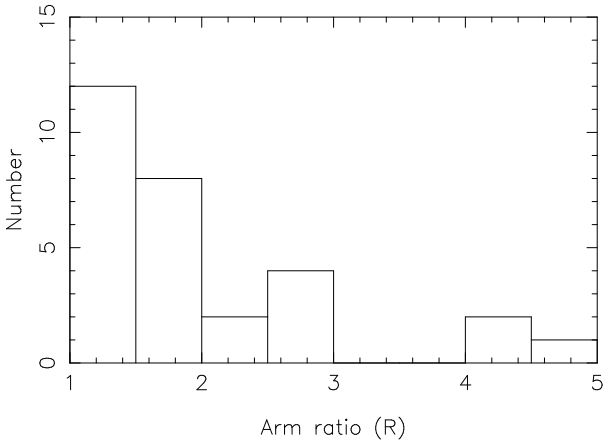

Figure 7. The arm ratio (R) distribution of 29 CSOs, with 78% completeness.

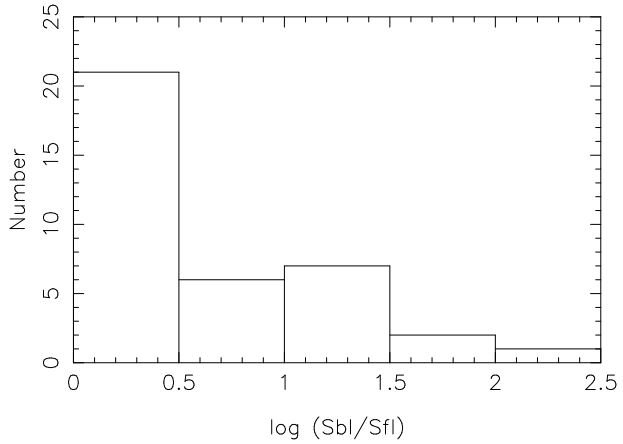

Figure 6. The flux density ratio (bright-lobe over faint-lobe) distribution of all the 37 CSOs.

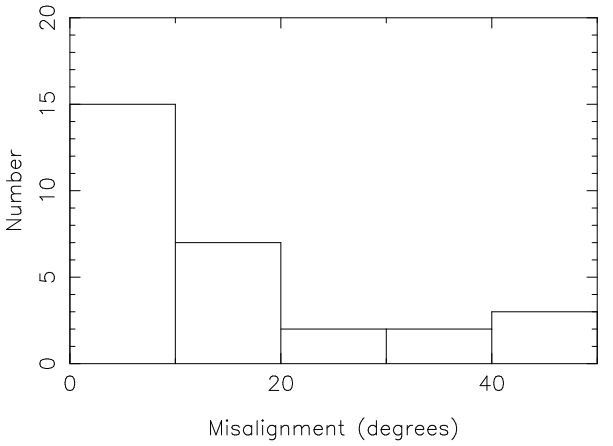

Figure 8. The misalignment angle (θ) distribution for 29 CSOs, 78% completeness.

In Figure 5 we show the ratio in flux densities between core and brightest lobe for 29 CSOs (78% complete). The remaining eight did not have a visible, properly located, core but we still show the upper limits (estimated from the maps). It turns out that a bright nucleus (ratio > 1 with respect to the bright lobe) is present in 11 (30%) of the sources (including the eight sources with upper limits in the statistics), in one case about 40 times brighter. At the other end, five sources (with upper limits) have a nucleus more than 100 times weaker than the brightest lobe. The median is $S_n/S_{bl\ (29)} = 0.7^{+0.8}_{-0.6}$.

We have studied the ratio in flux densities between the two opposed lobes for all the 37 CSOs (Figure 6): 27 (73%) have ratios < 10 (of which 21 (57% of the total) of 1 to 3) but one CSO has it as large as 113: in total, ten (27%) of the CSOs have > 10 ratios. The median is $S_{bl}/S_{fl\ (37)} = 2.2^{+2.1}_{-0.2}$.

A test of symmetry, which was adopted as definition for CSO/MSOs, is the arm length ratio (Figure 7). From the 29 CSOs (78% complete) with data (core located, from where each arm is measured) we find that none has an arm ratio above 4.6 and that two-thirds (20) have it smaller than two. The spread is not large and we have for the median: $R_{29} = 1.6^{+0.7}_{-0.4}$. Both in median and in distribution of arm ratios CSOs seem to lie somewhere between large FRII radio galaxies (symmetric) and CSS galaxies (asymmetric) — e.g. Saikia et al. (2003).

Although not formally established, it is generally understood that a CSO/MSO should be fairly well aligned, similarly to FRI/FRIIs. The inter-arm angular (ϕ) distribution for 29 CSOs (78% complete; they must have the core located in order to measure the angle) is plotted in Figure 8 but in the form of the misalignment angle (θ), obtained by subtracting ϕ from 180°. We have the following medians: $\phi_{29} = 171^{+5}_{-9}$ deg or $\theta_{29} = 9^{+9}_{-5}$ deg. We can then see that, as it was expected, CSOs are fairly well aligned sources, with $\theta \leq 20°$ for 22 (76%) of them.

For the 25 CSOs (68% complete) with measured redshifts, we plot, in Figure 9, their projected linear size (l) distribution. The median is $l_{25} = 0.14^{+0.07}_{-0.05}$ kpc. This indi-

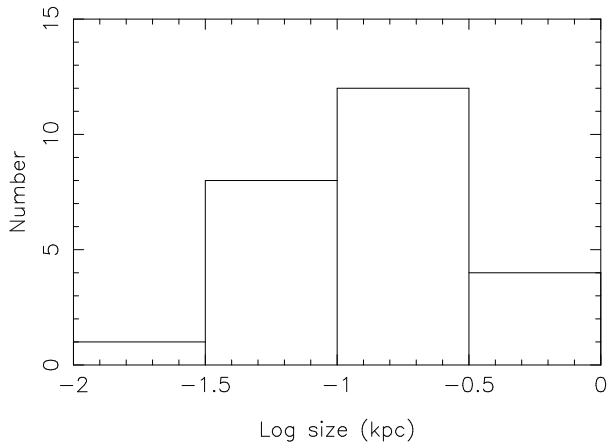

Figure 9. The projected linear size (l) distribution of 25 CSOs (68% complete).

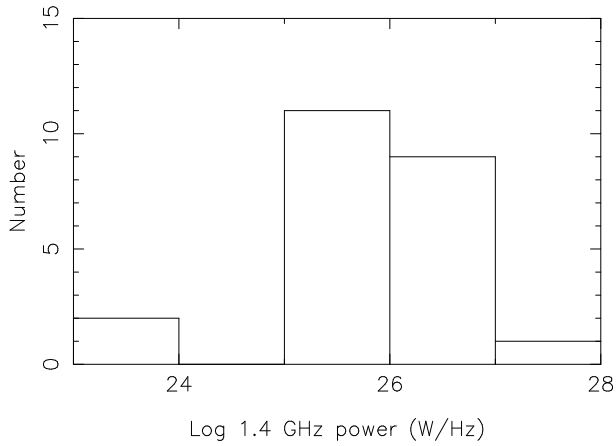

Figure 10. The 1.4 GHz power distribution for 23 CSOs, 62% completeness.

cates a lack of 0.3–1 kpc sources. In fact, from the Figure, we note that CSOs, in general, abound at < 0.3 kpc (21, 84% of the total) but are scarce over the rest of the way up to 1 kpc.

In Figure 10 we show the 1.4 GHz power distribution for the 23 CSOs (62% completeness) that have this information. The median [$\log L_{1.4} = 25.9^{+0.4}_{-0.2}$ (W/Hz)] and the distribution clearly reflect the fact that the selection and classification of CSOs, so far, has implied high-luminosity sources, namely with $L_{1.4} > 10^{25}$ (W/Hz). The bias is so strong that, using the formal definition at 178 MHz of the FRI/FRII border, with the help of the power extrapolation via α_{thin} and assuming a power decrease with the inverse square of size (e.g. Begelman 1996), only one of the 23 CSOs in Table 2 with enough information will be powerful enough to become a 1 Mpc size FRII: 4C+32.44. If we relax their future to 100 kpc FRIIs, only two more will be added to the list: B0428+205 and 4C+62.22. In any case, we have searched for a correlation between size and 1.4 GHz radio power but found none.

2.3 Flat-spectrum MSOs

We searched the literature and used the same criteria of Section 2.1 in order to identify $\alpha^{4.85}_{1.40} < 0.5$ flat spectrum MSOs. Only three were found (sizes on 1–15 kpc): 4C+34.07, a $z = 2.910$ QSO (Willott et al. 1998); NGC3894, a $z = 0.01075$ galaxy (de Vaucouleurs et al. 1991); B2151+174, a $z = 0.23024$ cD galaxy (Yee et al. 1996). Their spectral and morphological radio properties (with references) are summarized in Table 3.

3 CANDIDATE ∼KPC FLAT-SPECTRUM SYMMETRIC OBJECTS

3.1 The revised parent sample

Augusto et al. (1998) have selected, from the ∼ 4700 sources of JVAS+CLASS1, a parent sample containing sources with $|b^{II}| > 10^\circ$, $S_{8.4\,GHz} \geq 100$ mJy and[§] $\alpha^{4.85}_{1.40} < 0.5$ ($S_\nu \propto \nu^{-\alpha}$). However, their total of 1665 objects was short by about 78 sources[¶] because $\alpha^{4.85}_{1.40}$ was calculated from all kinds of catalogues. In order to obtain *same epoch* $\alpha^{4.85}_{1.40}$ we got all values from White & Becker (1992) and Gregory & Condon (1991), for the 1.40 GHz and 4.85 GHz frequencies, respectively[‖]. Sources without $\alpha^{4.85}_{1.40}$ information were also kept.

The revised parent sample now contains 1743 sources (Table 4), whose redshift and spectral index distributions are presented in Figures 11 and 12, respectively. We note that these distributions use the full sample rather than just a representative subsample (c.f. Augusto et al. 1998). A full discussion on the implications of the revision of the parent sample is made in Appendix A.

3.2 The 157-source sample

Although small-size (VLBI scale: 1–300 pc) CSOs had dedicated searches/surveys in order to find them (e.g. Peck & Taylor 2000), bringing the current number of confirmed cases to 37 (c.f. Table 2 and Figure 9), the problem is that large-scale CSOs and $\alpha < 0.5$ flat-spectrum MSOs (0.3–15 kpc size range; see also Table 3) have only seven confirmed cases. It was vital first, no doubt, to establish CSOs as new, worth of studying, objects and the VLBI efforts had the ideal impact, showing (many of) them as young sources. We believe that the time has come to start populating the 0.3–1 kpc size-range with CSOs, if we really want to learn

[§] Bondi et al. (1998) point out that at frequencies below ∼ 1 GHz, interstellar scintillation might induce extrinsic variability in extragalactic radio sources. Hence, our selection with $\alpha^{4.85}_{1.40}$ should be safe, as compared to other selections made with $\alpha^{high-\nu}_{0.3}$, likely more affected by such variability.

[¶] Globally. There is a further complication since some sources that are in the revised sample were not in the old one (e.g. B0218+357) and vice-versa.

[‖] It would be more tempting to use the NVSS/GB6 combination (1.4/4.85 GHz; Condon et al. 1998/Gregory et al. 1996), which would fill more blanks in Columns (4)–(6) of Tables 4 and 5. However, given that the observation epochs are ∼ 10 yrs apart, many such calculated spectral indices might not be trustworthy.

Table 3. The three confirmed MSOs from the literature. The description for each column is as in Table 2 (columns (10)–(18)). References for the radio maps on the three sources: Dallacasa et al. (1995); Beasley et al. (2002); Fomalont et al. (2000); Spencer et al. (1989); Taylor et al. (1994); Taylor et al. (1998); Augusto et al. (1998); Augusto et al. (2005).

(1) Source	**(2)** $\alpha_{1.40}^{4.85}$	**(3)** α_{thin}	**(4)** LAS ($''$) [l (kpc)]	**(5)** S_n/S_{bl}	**(6)** S_{bl}/S_{fl}	**(7)** R	**(8)** ϕ	**(9)** $L_{1.4}$
4C+34.07	0.41	0.3_s	$1.85^{1.7}$ (12.85) *	$11^{1.7}$	$6.7^{1.7}$	$1.2^{1.7}$	$174^{\circ\,1.7}$	26.8
NGC3894	−0.33	-0.2_3^5	6.54 (1.34)	6.0	3.4	1.0	180°	22.9
B2151+174	0.13	0.3_3	0.49 (1.58)	15	3.7	1.7	166°	25.2

Table 4. The parent sample of 1743 flat-spectrum ($\alpha_{1.40}^{4.85} < 0.5$) radio sources (extract only — the complete version can be found at CDS, ftp://cdsarc.u-strasbg.fr). Description of each column: **(1):** The source name (J2000.0); **(2,3):** position (J2000.0); **(4):** 1.40 GHz flux density from White & Becker (1992) — generally; < 110 mJy conservative upper limits are placed on some sources which were covered in the sky survey but were not detected down to the ∼ 100 mJy treshold; other limits are for sources not covered in the survey and observed with NVSS — Condon et al. 1998 (total flux density of all detected components within a 10′radius); **(5):** 4.85 GHz flux density from Gregory & Condon (1991); **(6):** spectral index, calculated from Columns (4) and (5) using the convention $S_\nu \propto \nu^{-\alpha}$; **(7):** redshift; **(8):** reference for the redshift; **(9):** note/comment.

(1) Name	**(2)** RA (2000)	**(3)** Dec (2000)	**(4)** $S_{1.40}$ (mJy)	**(5)** $S_{4.85}$ (mJy)	**(6)** $\alpha_{1.40}^{4.85}$	**(7)** z	**(8)** Ref.	**(9)** Note
J0457+067	04 57 07.7102	06 45 07.275	< 571	435	< 0.22	0.405	45	
J0458+201	04 58 29.8726	20 11 35.997	170	163	0.03			
J0459+024	04 59 52.0509	02 29 31.176	1752	1689	0.03	2.384	7	
J0501+139	05 01 45.2706	13 56 07.218	235	468	-0.55			
J0501+714	05 01 45.7829	71 28 33.977	< 110	148	< −0.23			
J0502+061	05 02 15.4466	06 09 07.507	1016	929	0.07	1.106	45	
J0502+136	05 02 33.2194	13 38 10.949	581	504	0.11			
J0503+020	05 03 21.1972	02 03 04.674	2118	1888	0.09	0.58457	21	
J0503+660	05 03 56.4447	66 00 31.503	< 110	158	< −0.29			
J0505+049	05 05 23.1850	04 59 42.723	659	964	-0.31	0.954	45	
J0505+641	05 05 40.9360	64 06 26.316	356	214	0.41			
J0508+845	05 08 42.3648	84 32 04.543						A

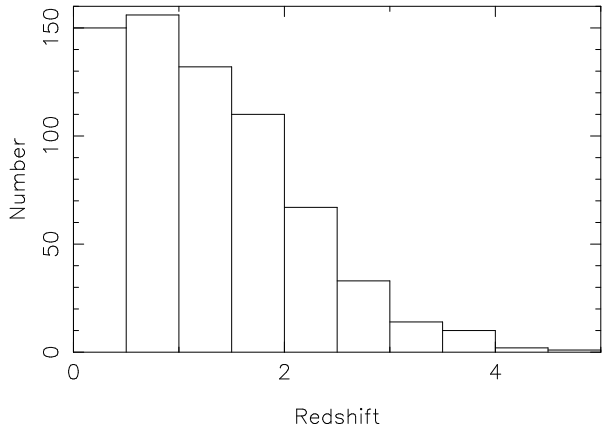

Figure 11. The redshift distribution of the 675 sources of the 1743-source parent sample which have such information (39% completeness).

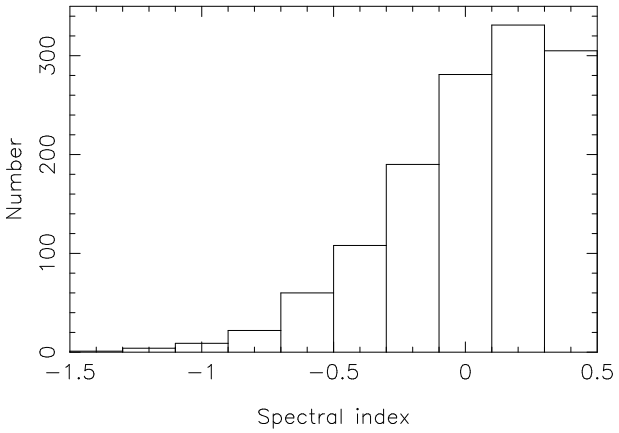

Figure 12. The 1.40–4.85 GHz spectral index distribution of the 1311 sources of the 1743-source parent sample which have such data (75% completeness).

about the full story of the small/young 1–300 pc CSOs evolution all the way into FRIIs or FRIs. In this respect, more flat-spectrum MSOs are also needed.

Augusto et al. (1998) presented 23 CSO/MSO candidates included in a 55-source sample selected from the parent sample by showing a greater than 25% decrease in their

8.4 GHz VLA-A visibilities (usually corresponding to strong radio features with <7:1 flux density ratio and $\gtrsim 0\farcs1$ apart; at $z > 0.2$, the projected linear size is $\gtrsim 0.3$ kpc). However, the 55-source sample was biased towards finding gravitational lenses: many sources were excluded from their final sample using a further surface brightness criterion in that sources with a bright and compact component plus other fainter and resolved components would be rejected (as well as any sources with dominant components $> 0\farcs3$ apart) — the full details are in Augusto (1996).

Since we now do not apply to the parent sample any of those extra criteria and only use the visibility criterion, we end up with a sample that includes 157 objects (including the 55 sources of Augusto et al. 1998) — Table 5, some of which are very extended objects. We do not claim that this sub-sample of 157 CSO/MSO candidates is complete since neither is JVAS for the reasons presented, e.g, in Augusto et al. (1998) and Patnaik et al. (1992a).

Using the same classification criteria as for building Table 2 (mentioned in Table 1), a literature search ruled out 61 sources as CSO/MSO candidates, also "rediscovering" nine of the CSO/MSOs in Table 2/Section 2.3 (including "CSO?" cases). We have discovered two new ~ 14 kpc MSOs (J0751+826, J1454+299) and two CSO/MSOs (4C+66.09, J2055+287; a redshift is needed for each, for final classification; the latter case can be an MSO only if its redshift is < 0.09).

An obvious test to our criteria would be to check how many of the northern hemisphere confirmed flat-spectrum ($\alpha^{4.85}_{1.40} < 0.5$) CSOs in Table 2 were not selected by us from the parent sample, and why. To identify them it is easy, since they are the ones that are both in Tables 2 and 4 and not in Table 5: they total to 13, of which 12 have sizes ≤ 40 mas, hence they would never have been selected by our criteria. Recalling that we typically can only identify sources that have, at least, two components $\gtrsim 0\farcs1$ apart and with $< 7:1$ flux density ratio at 8.4 GHz, as regards to the only remaining (B1413+135), although with a global size of $\sim 0\farcs18$, it has a very faint lobe ($S_n/S_{fl} \simeq 35$) while the bright lobe ($S_n/S_{bl} \simeq 1.6$) is too close to the nucleus ($\sim$35 mas). So, it could not have been selected.

In what follows we describe in detail the sources that refer to the text in Table 5:

J0013+778: This is a bright core large symmetric object (LSO), which has detailed information with 1.6 GHz VLBI (Polatidis et al. 1995) and 1.4 GHz VLA (Xu et al. 1995). We locate its core thanks to the JVAS map, since at 8.4 GHz with the VLA-A the middle VLBI component has the most inverted spectrum of all while the northeast component also shows a more modest inverted spectrum; the one of the southwest component is very steep. The overall size is about $8''$ in a north-south direction (thanks to further, weaker VLA 1.4 GHz components) which, at its redshift of 0.326, gives it ~ 32 kpc.

4C+36.01: This is a radio galaxy with an extended halo, giving it an overall size of ~ 40 kpc, as can be seen in a VLA 1.4 GHz map (Taylor et al. 1996b).

J0123+307: This source is a good example on why JVAS is not a complete sample. As explained (and imaged) in detail in Augusto (1996) this is, in fact, a VLBA point source (500:1 map) that had its position in error by an amount sufficient to cause bandwidth smearing and confuse our visibility selection criterion (see also Augusto et al. 1998; Patnaik et al. 1992a).

J0259+426: As for the previous source, this was also a JVAS failure and the selection was made erroneously. Although not quite a VLBI point source (it is a triple source ~ 15 mas in size — Henstock et al. 1995) it should never have been selected.

3C108: This is a triple source with a candidate core at the centre from a MERLIN 1.7 GHz map in Saikia et al. (1990). In JVAS, the 8.4 GHz VLA-A map confirms the central component as a core ($\alpha^{8.4}_{1.7} \simeq 0.2$) while the source redshift of 1.215 implies that its $5\farcs88$ angular size means a linear projected size of $\sim$40 kpc. Hence, this source is rejected.

J0654+427: Bondi et al. (2001) give two VLBI maps at different resolutions (and frequencies: 1.6 and 4.9 GHz) that leave no room for doubt that the structure is that of a core-jet source rather than a CSO/MSO: the brightest component in both images is the core since it has $\alpha^{4.9}_{1.6} = 0.0$ (using peak brightnesses), likely becoming inverted if model fitting is applied.

J0656+321: Yet another source that is an example of why JVAS is not a complete sample. As explained (and imaged) in detail in Augusto (1996) this is, in fact, a MERLIN point source (670:1 map) that had its position in error by an amount sufficient to cause significant bandwidth smearing (see also Augusto et al. 1998; Patnaik et al. 1992a).

J0751+826: Also presenting VLBI compact structure (Polatidis et al. 1995; Xu et al. 1995), with an easily identified core, the large scale structure of this source, easily seen in the VLA-A 8.4 GHz map of JVAS, looks like a $\sim 2''$ wide-angle tail. Its 1.991 redshift implies a global size of ~ 14 kpc, just at the border of still classifying it as an MSO.

J0815+019: This source is in the appendix of Augusto et al. (1998), discarded by them from the 55-source sample (due to an erroneous spectral index evaluation — see Section 3.1). It is now recovered into the 157-source sample. Augusto et al. (1998) presented a MERLIN 5 GHz map of the source. We must locate the core in future multi-frequency follow ups.

J0817+324: As explained (and imaged) in detail in Augusto (1996) this is, in fact, a MERLIN point source (500:1 map) that had its position in error by an amount sufficient to cause significant bandwidth smearing (see also Augusto et al. 1998; Patnaik et al. 1992a).

J0837+584: All evidence seems to point to a core-jet source. In addition to the JVAS map and visibility, hinting at a strong unresolved component plus a very weak and distant ($\sim 0\farcs6$ away) blob, the two frequency 1.6 and 5 GHz VLBI maps of Polatidis et al. (1995) and Xu et al. (1995) locate the nucleus as the westernmost component, with $\alpha^{5}_{1.6} = 0.15$ as opposed to the $\alpha^{5}_{1.6} = 1.4$ value of the other strong component ~ 8 mas away.

J0855+578: This source was observed with the VLBA at 5 GHz by Taylor et al. (2005). It has one of the lobes edge-brightened but the other is not so convincing. There is no core detected. We must find a core with higher frequency observations, or a more convincing structure to pass our strict criterion for a CSO confirmation; Taylor et al. (2005) have not managed to detect this (weak) source at 15 GHz.

4C+66.09: This source is in the appendix of Augusto

et al. (1998), discarded by them from the 55-source sample. It is now recovered into the 157-source sample. Augusto et al. (1998) presented a MERLIN 5 GHz map of the source which leaves no room for doubt that this source is either a CSO or an MSO, depending on its unknown redshift: edge-brigthening is seen in both lobes, although no core is detected. VLBA observations have been conducted for this source at 1.7, 4.8 and 15 GHz (Rossetti et al. 2005) confirming the classification and finding hotspots at both ends, although the nucleus still remains undetected.

4C+55.17: The multi-frequency maps of Reid et al. (1995) and the source redshift of 0.909 imply a large size ($\sim$ 53 kpc), although the source is symmetric indeed (an LSO).

J1015+674: Augusto (1996) shows it as a MERLIN point source (300:1 map) that had its position in error by an amount sufficient to cause significant bandwidth smearing (see also Augusto et al. 1998; Patnaik et al. 1992a).

J1041+525: This is a well-studied large scale quasar ($\sim$ 150 kpc in size), easily seen also in VLBI scales (e.g. Henstock et al. 1995; Taylor et al. 1996b).

J1058+198: With a global size of $\sim$ 420 kpc (62″at a redshift of 1.11), this is a very large source, possibly a radio galaxy (e.g. Hooimeyer et al. 1992).

J1110+440: Augusto (1996) shows it as a core-jet source (a very compact and strong nucleus and an extended, 50 times weaker, jet).

J1306+801: This is a very large triple source ($\sim$110 kpc — Taylor et al. 1996b), possibly an LSO, since the core appears to be located in the middle component (from multi-frequency data).

J1324+477: Augusto (1996) shows it as a point source, in a 200:1 MERLIN 5 GHz map, so this source was erroneously selected due to bandwidth smearing.

J1424+229: This is a well known arcsecond-scale gravitationally lensed multiple-image system (e.g. Patnaik et al. 1992b).

J1440+383: This source is in the appendix of Augusto et al. (1998), discarded by them from the 55-source sample and now recovered into the 157-source sample. Augusto et al. (1998) presented a MERLIN 5 GHz map of this double source for which its 8″ separation translates into $\sim$ 50 kpc at the source redshift of 1.775.

J1454+299: This source is in the appendix of Augusto et al. (1998), discarded by them from the 55-source sample and now recovered into the 157-source sample. Augusto et al. (1998) presented a MERLIN 5 GHz map of the source which leaves no room for doubt that this source is an MSO, given the edge-brigthening in both lobes and the presence of a central compact "core"; the overall size of $\sim$2.″5 corresponds to $\sim$ 14 kpc at the source redshift of 0.58.

J1504+689: Lara et al. (2001) show this source as a large-scale giant radio QSO, with a size of 1.16 Mpc.

J1526+099: A confirmed LSO (from the VLA-A maps of JVAS at 8.4 GHz and of Hintzen et al. (1983) at 1.4 GHz) which, given its redshift of 1.358 and from its angular size of $\sim$ 15.″5, has a global size of $\sim$ 110 kpc.

Arp220: This is a very well known radio galaxy with ultraluminosity at IR wavelengths, presenting a double radio/IR nucleus (Norris 1988; Graham et al. 1990) and also maser emission. Too many observations at all wavelengths exist for this source to mention here, so just as essential examples we cite Emerson et al. (1984); Soifer et al. (1984); Norris et al. (1985); Shaya et al. (1994); Heckman et al. (1996); Scoville et al. (1998); Clements et al. (2002). It is not a CSO/MSO since it is thought that most of its radio emission comes from strong starburst activity (e.g. Rovilos et al. 2003).

4C+49.26: As already pointed out by Augusto et al. (1998) this source is an LSO with a 6″ size which, at its redshift of 0.7, makes it $\sim$ 36 kpc in total.

J1607+158: This is a core-jet source, from VLBI (Beasley et al. 2002) up to 8.4 GHz VLA-A scales (JVAS).

4C+12.59: From several multi-frequency maps (Saikia et al. 1990; Lonsdale et al. 1998; Dallacasa et al. 1998) it is still not clear whether this source is a core-jet or an LSO. From our point of view this is irrelevant, since its angular size of 3.″3 and redshift of 1.795 make it $\sim$ 24 kpc in size.

J1715+217: A recent VLBA map on this source (Gurvits et al. 2006, in prep.) shows it as a core with a jet containing a strong feature about $\sim$ 60 mas from the core. The VLA-A 8.4 GHz visibilities, however, suggest larger scale structure as well. Future MERLIN 5 GHz observations should find it.

J1749+431: All extant multi-frequency maps (Henstock et al. 1995; Taylor et al. 1996b; Beasley et al. 2002) strongly suggest that this source has a core-jet structure.

J1753+093: All evidence seems to identify this radio source with a galactic star (Thompson et al. 1990).

NGC6521: Condon et al. (2002) find it likely that this source has a core plus two lobes on each side, with an overall size of 5′, giving it a size of $\sim$ 150 kpc at its 0.027462 redshift.

NGC6572: This source is a galactic planetary nebula (e.g. Condon & Kaplan 1998).

J2055+287: This source is in the appendix of Augusto et al. (1998), discarded by them from the 55-source sample. It is now recovered into the 157-source sample. Augusto et al. (1998) presented a VLA 1.4 GHz map of the source which shows it with a clear structure containing edge-brightened lobes. If it lies at a redshift closer than 0.09 it still can be classified as an MSO (size $<$ 15 kpc).

J2234+361: This source is in the appendix of Augusto et al. (1998), discarded by them from the 55-source sample and now recovered into the 157-source sample. Augusto et al. (1998) presented both MERLIN and VLBA 5 GHz maps of this source after which there is no doubt to classify its structure as a core-jet.

3.3 Statistics

In Figures 13 and 14 we plot, respectively, the redshift (z) and spectral index ($\alpha_{1.40}^{4.85}$) distributions for the 157-source sample (which have different completenesses). The compared statistics of this new sample with the previous 55-source sample of Augusto et al. (1998) are discussed in Appendix A. Relevant here is the comparison with the new 1743-source parent sample (Figure 11 vs. 13; Figure 12 vs. 14), with results shown in Table 6. The completenesses are similar for both samples. This similarity, in the redshift case, is not surprising since the two samples have the same flux density lower limit. The completeness similarity in the case of the spectral index merely reflects that we are not biasing our selection towards "better known" or brighter sources (which is good, since we want a morphological-only difference): the proportion of sources that are too weak to be

Table 5. The sample of 157 flat-spectrum ($\alpha_{1.40}^{4.85} < 0.5$) radio sources. The columns are as in Table 4, except that; i) column (7) only exists here (its caption is as in column (12) of Table 2 with an additional subscript: f — flattening of the spectrum at high-ν); ii) in column (10) we give comments on the status of the candidate: CSO/MSO (?) — (not yet) confirmed CSO/MSO — see text (t) or Table 2/Section 2.3 (S) for more details; OUT — ruled out, see why in text or in Augusto et al. (1998) for the sources marked with a "55" superscript; OBS — data exist (need processing/interpreting); ? — the cases that will need observations in the future for the first step in the classification of their structure; MERLIN/VLBI — sources that have adequate structure but lack multi-frequency observations to confirm core location (see text or Augusto et al. (1998) for the sources marked with a "55" superscript). For this table, also, we give here the redshift references (Column (9)) with the same code numbers as in Table 4: 3– White et al. (1993); 7– Hewitt & Burbidge (1989); 9– Wills & Wills (1976); 10– Xu et al. (1994); 13– Stickel & Kuhr (1993); 17– Vermeulen & Taylor (1995); 18– Goncalves et al. (1998); 20– Hewett et al. (1995); 22– Hook et al. (1996); 23– Henstock et al. (1997); 25– Marcha et al. (1996); 37– Miller & Owen (2001); 41– Parkes Catalogue (1990), Australia Telescope National Facility, Wright & Otrupcek, (Eds); 45– Drinkwater et al. (1997); 62– Allington-Smith et al. (1988); 63– Burbidge & Crowne (1979); 64– Stickel & Kuhr (1996); 65– Puchnarewicz et al. (1992); 66– Stickel et al. (1996); 67– Le Borgne et al. (1991); 68– Baldwin et al. (1973); 69– Unger et al. (1986); 70– Sargent (1973); 71– Vermeulen et al. (1996); 73– Falco et al. (1998); 81– Hewitt & Burbidge (1991); 86– de Vaucouleurs et al. (1991); 103– Patnaik et al. (1992b); 104– Hook & McMahon (1998); 108– Wegner et al. (1999); 113– Dondi & Ghisellini (1995); 141– Sloan Digital Sky Survey (`www.sdss.org`); 142– Cohen et al. (2003); 143– Gorshkov et al. (2003); 144– Magliocchetti et al. (2004); 145– Sowards-Emmerd et al. (2003).

(1) Name	**(2)** RA (2000)	**(3)** Dec (2000)	**(4)** $S_{1.40}$ (mJy)	**(5)** $S_{4.85}$ (mJy)	**(6)** $\alpha_{1.40}^{4.85}$	**(7)** α_{thin}	**(8)** z	**(9)** Ref.	**(10)** Notes
J0000+393	00 00 41.5259	39 18 04.172	220	138	0.38	0.4_3			?
J0009+400	00 09 04.1750	40 01 46.724	569	333	0.43	0.5	1.83	7	OBS
J0013+778	00 13 11.6992	77 48 46.620	2203			$0.5_3^{0.1}$	0.326	10	OUT
J0020+430	00 20 49.9798	43 04 38.329	363	253	0.29	0.5			?
J0026+351	00 26 41.7238	35 08 42.285	819	453	0.48	0.4_3	0.333	13	?
J0036+318	00 36 48.1263	31 51 14.532	256	148	0.44	0.6_3			?
4C+36.01	00 37 46.1437	36 59 10.928	879	482	0.48	0.6_s	0.366	17	OUT
4C+12.05	00 38 18.0173	12 27 31.252	1002	670	0.32	0.7_f	1.395	18	?
J0048+319	00 48 47.1438	31 57 25.094	270	254	0.05	0_v	0.015	69	CSO (S)
J0112+203	01 12 10.1864	20 20 21.789	407	247	0.40	0.6_3	0.746	7	?
J0115+521	01 15 56.8741	52 09 13.034	328	206	0.37	0.7			MERLIN^{55}
J0119+321	01 19 34.9991	32 10 50.013	2826	1571	0.47	$0.4^{0.4}$	0.0592	70	CSO (S)
J0123+307	01 23 02.2783	30 44 06.847	126	184	−0.30				OUT
J0129+147	01 29 55.3484	14 46 47.843	706	536	0.22	0.6_f	1.62985	141	OUT^{55}
J0138+293	01 38 35.3234	29 22 04.544	324	184	0.46	0.5_3			?
J0209+724	02 09 51.7921	72 29 26.669	842	560	0.33	0.4	0.895	71	MERLIN^{55}
J0221+359	02 21 05.4702	35 56 13.722	1456	1498	−0.02	0.3	0.944	142	OUT^{55}
J0227+190	02 27 53.3347	19 01 14.082	292	160	0.48	0.5_3			MERLIN/VLBI^{55}
J0237+437	02 37 01.2149	43 42 04.191	431	246	0.45	$0.5_3^{0.4}$			CSO (S)
J0255+043	02 55 55.4349	04 19 40.588	435	278	0.36	0.5_3			?
J0259+426	02 59 37.6753	42 35 49.908	616	366	0.42	0.2	0.867	17	OUT
J0308+699	03 08 27.8276	69 55 58.900	228	205	0.09	0.3_f			OBS
J0348+087	03 48 10.4178	08 42 08.873	248	192	0.21	0.5_3			OUT^{55}
J0354+801	03 54 46.1258	80 09 28.816	818			0.4			?
J0355+391	03 55 16.5912	39 09 09.824	160	191	−0.14	0.4			OUT^{55}
J0402+826	04 02 12.6736	82 41 35.103							CSO (S)
3C108	04 12 43.6683	23 05 05.468	1293	1000	0.21	$0.6_{v,f}$	1.215	7	OUT
J0420+149	04 20 51.0857	14 59 15.634	460	310	0.32	0.5_3			OUT^{55}
4C+68.05	04 26 50.0654	68 25 52.955	<454	244	<0.50	0.6			?
J0431+206	04 31 03.7585	20 37 34.189	3611	2811	0.20	0.6_s^1	0.219	41	CSO (S)
J0431+175	04 31 57.3798	17 31 35.792	429	270	0.37	0.4_3			OUT^{55}
J0458+201	04 58 29.8726	20 11 35.997	170	163	0.03	$0.6_{3,v}$			OBS
4C+10.16	05 16 46.6463	10 57 54.773	1207	734	0.40	0.5	1.580	143	?
J0532+013	05 32 08.7760	01 20 06.330	258	153	0.42	0.4_3			OUT^{55}
J0600+630	06 00 27.0161	63 04 07.481	<110	114	< −0.02				?
J0626+621	06 26 42.2118	62 11 23.514	195	134	0.30	0.6_3			?
J0639+351	06 39 09.5887	35 06 22.543	346	233	0.32	0.4			?
J0641+356	06 41 35.8542	35 39 57.623	340	197	0.44	$0.5^{0.1}$			MERLIN^{55}
J0653+646	06 53 53.7227	64 38 13.176	178	130	0.25	0.4_3			?
J0654+427	06 54 43.5263	42 47 58.728	188	188	0.00	0.2	0.126	25	OUT
J0656+321	06 56 40.8892	32 09 32.554	<110	217	< −0.54				OUT
J0735+236	07 35 59.9293	23 41 02.764	878	552	0.37	0.5			MERLIN/VLBI^{55}
J0751+826	07 50 57.7640	82 41 58.032	1815			0.5_f	1.991	10	MSO (t)
J0752+581	07 52 09.6792	58 08 52.256	203	212	−0.03	0.0_f	2.94	3	OBS
J0757+611	07 57 44.6933	61 10 32.764	246	195	0.19	$0.3_{3,s}$			?
J0803+640	08 03 52.1595	64 03 14.364	292	221	0.22	0.2			?
J0815+019	08 15 58.6371	01 55 55.820	<110	280	< −0.75	0.7			MERLIN

(1) Name	(2) RA (2000)	(3) Dec (2000)	(4) $S_{1.40}$ (mJy)	(5) $S_{4.85}$ (mJy)	(6) $\alpha_{1.40}^{4.85}$	(7) α_{thin}	(8) z	(9) Ref.	(10) Notes
J0817+324	08 17 28.5455	32 27 02.928	<564	585	< -0.02	0.4_f			OUT
J0817+556	08 17 41.0199	55 37 33.283	178	244	-0.25	0.3			?
J0822+708	08 22 16.7649	70 53 07.978	436	274	0.37	$0.7^{0.1}$			MERLIN/VLBI[55]
J0822+080	08 22 33.1537	08 04 53.523	<110	204	< -0.49				MERLIN/VLBI[55]
J0824+392	08 24 55.4837	39 16 41.898	1381	1012	0.25	0.5_f	1.216	9	OUT[55]
J0827+354	08 27 38.5891	35 25 05.081	866	746	0.12	$0.5_{3,f}$	2.249	62	MERLIN[55]
J0832+278	08 32 19.6581	27 52 43.879	467	274	0.43	0.5_3			OBS
J0834+555	08 34 54.9026	55 34 21.086	7741	5780	0.24	1.1_s	0.242	63	OUT[55]
J0837+584	08 37 22.4100	58 25 01.844	597	669	-0.09	0_v	2.101	7	OUT
J0855+578	08 55 21.3575	57 51 44.082	<110	279	< -0.74	0.7_3			VLBI
J0901+671	09 01 58.7485	67 07 32.225	<219	100	<0.64				?
J0908+418	09 08 35.8623	41 50 46.204	<110	207	< -0.50	0.4_3	0.7325	73	OUT[55]
J0911+861	09 11 37.7924	86 07 33.504				0.7_3			?
J0915+209	09 15 08.7822	20 56 07.367	257	191	0.24	0.4_f			?
4C+58.18	09 16 59.7887	58 38 49.349	<1478	313	<1.25	1.0			?
J0917+737	09 17 28.0923	73 43 13.460	213	161	0.23	0.5_3			?
J0921+716	09 21 23.9433	71 36 12.417	384	292	0.22	0.6_v	0.594	64	OUT[55]
3C225A	09 42 08.4797	13 51 54.229	<110	376	< -0.98	0.0_3	1.565	81	OBS
4C+66.09	09 49 12.1652	66 14 59.587	2223	1407	0.37	$0.6_s^{0.4}$			CSO/MSO (t)
4C+55.17	09 57 38.1825	55 22 57.734	3000	2270	0.22	0.4_v	0.909	7	OUT
J1002+122	10 02 52.8457	12 16 14.588	179	285	-0.37	$0.0_{3,f}$			?
J1003+260	10 03 42.2292	26 05 12.903	491	274	0.47	0.4_v			?
J1005+240	10 05 07.8712	24 03 38.003	209	146	0.29				?
J1006+172	10 06 31.7650	17 13 17.104	497	337	0.31	0.5_3			OUT[55]
J1013+284	10 13 03.0002	28 29 10.926	612	331	0.49	$0.6_3^{0.1}$			MERLIN/VLBI[55]
J1015+494	10 15 04.1358	49 26 00.692	382	286	0.23	0.3	0.2	65	OUT[55]
J1015+674	10 15 38.0161	67 28 44.442	<110	117	< -0.05				OUT
J1034+594	10 34 34.2393	59 24 45.846	164	142	0.12	$0.5_{3,f}$	(2.13069)**	141	OBS
J1035+568	10 35 06.0207	56 52 57.960	273	227	0.15	$0.6_{3,f}$	1.855420††	141	?
J1041+525	10 41 46.7800	52 33 28.217	713	709	0.00	0.2	0.677	7	OUT
J1058+198	10 58 17.8992	19 51 50.902	2310	1678	0.26	0.5_f	1.11	7	OUT
J1101+242	11 01 23.5143	24 14 29.517	416	231	0.47	$0.6_3^{0.1}$			MERLIN[55]
J1108+020	11 08 46.35	02 02 43	928	678	0.25	0.4_v	0.157/0.158	45,141,144	?
J1110+440	11 10 46.3458	44 03 25.938	373	297	0.18	0.2			OUT
4C+20.25	11 25 58.7440	20 05 54.381	<110	759	< -1.55	0.5_v	0.133	25	?
J1132+005	11 32 45.6189	00 34 27.821	472	358	0.22	0.5_v	1.22270	141	?
J1141+497	11 41 54.8254	49 45 06.564	157	98	0.38	0.6_3			?
J1145+443	11 45 38.5190	44 20 21.918	438	245	0.47	0.3	0.3	22	OUT[55]
J1153+092	11 53 12.5524	09 14 02.312	737	500	0.31	0.5_v	0.698	9	OUT[55]
J1159+583	11 59 48.7733	58 20 20.306	<1557	369	<1.16	$0.7_{3,s}$			?
J1213+131	12 13 32.1412	13 07 20.373	1486	894	0.41	0.4	1.141	20	OBS
J1214+331	12 14 04.1129	33 09 45.556	1196	649	0.49	$0.3_s^{0.4}$	1.598	9	OUT[55]
J1215+175	12 15 14.7215	17 30 02.250	836	620	0.24	0.6_v			MERLIN/VLBI[55]
J1224+435	12 24 51.5059	43 35 19.282	393	235	0.41	0.3	1.872	145	?
J1226+096	12 26 25.4693	09 40 04.432	895	524	0.43	0.7			?
J1235+536	12 35 48.2529	53 40 04.839	392	215	0.48	0.5	1.97193	141	MERLIN[55]
J1239+075	12 39 24.5908	07 30 17.225	435	674	-0.35	0.0	0.4	7	OBS
J1243+732	12 43 11.2156	73 15 59.259	518	345	0.33	0.6_s	0.075	25	OUT[55]
J1244+879	12 44 06.7918	87 55 08.093				0.3_3			?
J1306+801	13 06 05.7164	80 08 20.543	862				1.183	71	OUT
J1319+196	13 19 52.0736	19 41 35.481	672	3866	0.45	0.5_3			OUT[55]
J1324+477	13 24 29.3413	47 43 20.624	188	237	-0.19	-0.1	2.26	22	OUT
J1334+092	13 34 19.5624	09 12 00.366	360	266	0.24	0.4_3			?
J1344+339	13 44 37.1019	33 55 46.195	262	154	0.43	0.4			OUT[55]
J1344+791	13 44 55.7307	79 07 10.834	370						?
J1411+592	14 11 21.9856	59 17 04.302	326	184	0.46	0.6	1.725	73	?
J1424+229	14 24 38.0940	22 56 00.590	220	503	-0.67		3.62	103	OUT
J1437+636	14 37 41.3537	63 40 05.772	<110	237	< -0.61				?
J1440+383	14 40 22.3365	38 20 13.627	1025	944	0.07	0.1	1.775	71	OUT

$\star\star$ If the identification is a QSO $\sim 9''$ away.
†† The previous redshift measurement (z=0.577) by Perlman et al. (1998) is very different.

(1) Name	(2) RA (2000)	(3) Dec (2000)	(4) $S_{1.40}$ (mJy)	(5) $S_{4.85}$ (mJy)	(6) $\alpha_{1.40}^{4.85}$	(7) α_{thin}	(8) z	(9) Ref.	(10) Notes
4C+13.53	14 42 04.0423	13 29 16.067	545	341	0.38	0.6			?
J1454+299	14 54 32.3006	29 55 58.110	822	460	0.47	0.5_f	0.58	7	MSO (t)
J1504+689	15 04 12.7748	68 56 12.830		229			0.318	7	OUT
J1507+103	15 07 21.8815	10 18 44.988	368	227	0.39	0.5_3			MERLIN/VLBI[55]
J1526+099	15 26 46.3484	09 59 10.538	430	346	0.17	0.7	1.358	7	OUT
J1530+059	15 30 28.4444	05 55 13.030	552	308	0.47	0.6_3			OBS
Arp220	15 34 57.2240	23 30 11.608	302	204	0.32	$0.3_s^{0.1}$	0.018126	86	OUT
4C+49.26	15 47 21.1384	49 37 05.810	936	549	0.43	0.5_s	0.7	22	OUT
J1607+158	16 07 06.4309	15 51 34.503	603	512	0.13	0.6_f	0.357	113	OUT
J1617+041	16 17 13.5894	04 08 41.674	372	439	−0.13	0.3_3			?
J1630+215	16 30 11.2359	21 31 34.379	300	245	0.16	$0.6_{3,v}$			MERLIN[55]
4C+12.59	16 31 45.2469	11 56 02.991	1628	954	0.43	0.6	1.795	7	OUT
J1635+599	16 35 37.6511	59 55 15.097	234	218	0.06				?
J1640+123	16 40 47.9384	12 20 02.108	2066	1292	0.38	$0.6^{0.3}$	1.152	66	OUT[55]
J1644+053	16 44 56.0829	05 18 37.064	659	393	0.42	0.5_3			OUT[55]
J1706+523	17 06 00.9421	52 18 42.748		164					?
J1713+492	17 13 35.1484	49 16 32.548	260	216	0.15	0.4_f	1.552	73	?
J1715+217	17 15 21.2517	21 45 31.709	580	327	0.46	0.5_3	4.011	104	VLBI
J1722+561	17 22 58.0083	56 11 22.320	219	132	0.41	0.7			OUT[55]
J1746+260	17 46 48.2909	26 03 20.343	385	261	0.31	0.3_v	0.147	25	OUT[55]
J1749+431	17 49 00.3604	43 21 51.289	340	367	−0.06	0.2			OUT
J1751+509	17 51 32.5892	50 55 37.847	310	192	0.39	0.6	0.3284	73	OBS
J1752+455	17 52 26.1411	45 30 59.120	<223	104	<0.62				?
J1753+093	17 53 02.5264	09 20 02.982	883	514	0.44	0.5_f	0‡‡		OUT
NGC6521	17 55 48.4397	62 36 44.119	<110	198	< −0.47	0.6_3	0.027462	108	OUT
J1755+049	17 55 51.1535	04 54 52.566		244					?
J1759+464	17 59 41.7970	46 27 59.906	<110	124	< −0.09				?
J1803+036	18 03 56.2829	03 41 07.575		250					CSO? (S)
NGC6572	18 12 06.2100	06 51 13.382	495	1251	−0.75		0§§		OUT
J1814+412	18 14 22.7082	41 13 05.605	644	534	0.15	0.4	1.564	23	OUT[55]
J1829+399	18 29 56.5203	39 57 34.690	127	353	−0.82				?
J1857+630	18 57 29.1989	63 05 30.043	263	164	0.38	0.6			OUT[55]
J1928+682	19 28 20.5502	68 14 59.247	533	319	0.41	$0.5^{0.3}$			CSO? (S)
J1947+678	19 47 36.2599	67 50 16.928	264	165	0.38	0.5_3			CSO? (S)
J2007+748	20 07 04.3881	74 52 25.398	283	262	0.06	0.2_3			?
J2035+583	20 35 23.7535	58 21 18.759	313	220	0.28	0.3_s			OBS
J2045+741	20 45 42.8810	74 09 54.800	223	128	0.45				?
J2055+287	20 55 30.5466	28 47 38.347		232		0.7_3			MSO? (t)
J2102+666	21 02 36.6376	66 36 34.217		76					OUT[55]
J2114+315	21 14 50.4610	31 30 21.183	440	255	0.44	0.5_3			OUT[55]
J2144+190	21 44 57.7115	19 05 18.945	305	222	0.26	0.5_3			?
J2153+126	21 53 04.6587	12 41 05.211	422	264	0.38	0.5_3	2.22278	141	OUT[55]
J2153+176	21 53 36.8267	17 41 43.726	282	241	0.13	0.3	0.231	67	MSO (S)
J2204+046	22 04 17.6522	04 40 02.007	784	747	0.04	$0.5_{v,f}$	0.028	9	OUT[55]
J2207+392	22 07 46.0720	39 13 50.353	445	294	0.33	0.6			OUT[55]
J2213+087	22 13 21.7374	08 47 29.951	226	208	0.07	$0.4_{3,f}$			OUT[55]
J2217+204	22 17 15.8391	20 24 48.970	408	221	0.49	0.6_3			?
J2234+361	22 34 02.9764	36 11 00.333		141					OUT
J2250+143	22 50 25.3434	14 19 52.044	2127	1177	0.48	0.4	0.237	68	OUT[55]
J2344+278	23 44 37.0573	27 48 35.521	<110	148	< −0.23		0.0573	37	?
J2347+115	23 47 36.4062	11 35 17.893	313	201	0.36	0.5_3			MERLIN[55]

‡‡ This is a galactic star (see text).
§§ This is a galactic planetary nebulae (see text).

found on one (or both) of the White & Becker (1992) and Gregory & Condon (1991) catalogues is the same.

As regards as the redshift distributions, the difference is obvious by eye, with the 157-source sample containing more low-z sources than the parent sample. Furthermore, the latter has a smooth redshift distribution, roughly flattening around $z \sim 0.7$ and having an average redshift coincident with that of other flat spectrum radio source samples ($<z> \simeq 1.2$; Munoz et al. 2003). The median values also suggest a selection of the closest radio sources (0.88 vs. 1.12), albeit

Table 6. Comparison of the redshift (z) and spectral index distributions ($\alpha_{1.40}^{4.85}$) between the parent sample and the 157-source sample. The medians are indicated with their asymmetric errors (95% conf. level). We also give the number of sources for this calculation in each case (#) and the correspondent completeness to the whole sample. Finally, we indicate the Figures where the histograms are plotted.

sample	z (median)	#	comp.	Fig.	$\alpha_{1.40}^{4.85}$	#	comp.	Fig.
parent	$1.12^{+0.11}_{-0.10}$	675	39%	11	$0.08^{+0.03}_{-0.01}$	1311	75%	12
157-source	$0.88^{+0.34}_{-0.48}$	66	43%	13	$0.32^{+0.05}_{-0.07}$	123	78%	14

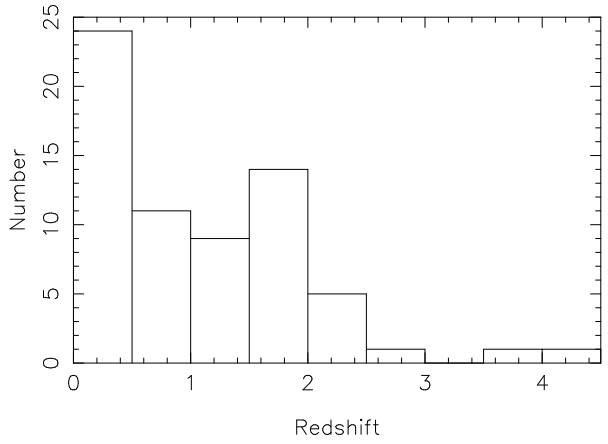

Figure 13. The redshift distribution of the 66 sources of the 157-source sample (minus two galactic sources) which have such information (43% completeness).

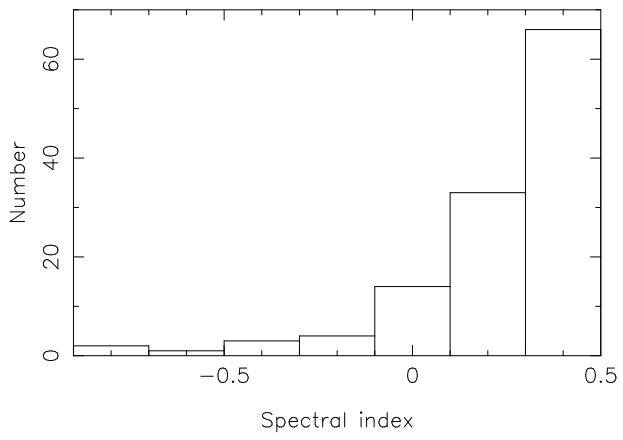

Figure 14. The 1.40–4.85 GHz spectral index distribution of the 123 sources of the 157-source parent sample which have such data (78% completeness).

with intersecting values, within the 95% conf. level errors. More formally, we have applied a KS-test to compare the two distributions and reject the hypothesis that they are similar at the 95% confidence level.

As for the spectral indices distributions we have, again, a smooth distribution for the parent sample (roughly flattening at $\alpha_{1.40}^{4.85} \simeq 0.2$) while for the 157-source sample the distribution is also smooth but still rising when it reaches the limit of $\alpha_{1.40}^{4.85} = 0.5$. This time, the distributions are clearly different by eye and medians (whose errors do not overlap). We performed the formal KS-test to compare both distributions and rejected the hypothesis that they are similar at the 99.9% confidence level. This result is similar to the one of Augusto et al. (1998) and also similarly explained by the fact that we are selecting resolved sources from the parent sample and this (normally) implies steeper spectrum sources.

4 SUMMARY

In what follows we briefly summarize the main conclusions from this paper:

- In order to understand the origin and evolution of extragalactic radio sources in the context of the standard model of AGN, several VLBI searches have been conducted trying to identify the youngest such sources ($\lesssim 10^3$ yrs), of which compact symmetric objects (CSOs) are the most serious contenders. Ideally, we should also follow the evolutionary track at later stages, by identifying somewhat older sources ($\sim 10^4$–10^5 yrs), possibly medium symmetric objects (MSOs). In this paper we summarize all confirmed cases of CSOs that we found from the literature, which total to 37, and three $\alpha_{1.40}^{4.85} < 0.5$ flat spectrum MSOs.
- By studying the sample of the currently confirmed 37 CSOs we conclude the following (the completeness of the statistics is $\geq 62\%$ but beware that the sample might not be representative of the CSO class due to the heterogeneous surveys from where the sources were selected): **i)** 85% of the optical hosts are galaxies, typically residing at $z \lesssim 0.5$; the remaining are quasars, with a large spread in redshift range; **ii)** most CSOs have flat radio spectra (70% with $\alpha_{1.40}^{4.85} < 0.5$; 56% with $\alpha_{thin} < 0.5$); **iii)** most (17, 59%) CSOs follow the "classical" (Wilkinson et al. 1994; Conway et al. 1994) definition where the brightness of the nucleus is $< 10\%$ of the one of the brightest lobe; one-third of the CSOs present nuclear components that are brighter than the brightest of the two opposed lobes — is this evidence for boosting?; **iv)** all CSO/MSOs were defined to have arm length ratios $R \leq 10$ (for symmetry); the maximum value on the present sample is $R = 4.6$, with 90% (all but three) having $R \leq 3.0$; **v)** 73% of the CSO/MSOs also present symmetry in the flux density ratios between the two lobes (≤ 10); however, this ratio can be as large as 113, among the remaining; **vi)** 76% of CSO/MSOs have well aligned opposing structures ($\theta \leq 20^\circ$) but values as large as $\theta = 46^\circ$ can be found; **vii)** CSOs have a median linear projected size of $0.14^{+0.07}_{-0.05}$ kpc, with 84% smaller than 0.3 kpc.
- The aim of the series of papers starting with this one

is to improve, many times, the number of confirmed large CSOs and of flat-spectrum MSOs (0.3–15 kpc), which currently sits at six. In this paper, in particular, we present a sample of 157 sources, drawn from a parent sample of 1743 flat spectrum ($\alpha_{1.40}^{4.85} < 0.5$) sources by selecting the ones with radio structure on $\gtrsim 0\farcs1$ scales. This resulted in the selection of the lowest redshift and steepest spectrum sources including $\gtrsim 0.3$ kpc CSO/MSO candidates. Although we have immediately rejected, based on literature information, 61 of the sources, 83 are still left with data either to be analysed or to be gathered. As for the remaining thirteen sources, nine were already listed as CSOs/flat-spectrum MSOs from the literature and are, thus, a good quality control for our selection. As for the final four, 4C+66.09 is a CSO/MSO (needs a redshift to identify which type exactly); J0751+826 and J1454+299 are $\sim$ 14 kpc MSOs; J2055+287 might be an MSO too, if at $z < 0.09$.

ACKNOWLEDGMENTS

The authors acknowledge an anonymous referee, whose comments helped to improve this paper, and also support from the Fundação para a Ciência e a Tecnologia (FCT) under the ESO programme: PESO/P/PRO/15133/1999. We thank Daniele Dallacasa for information on one source, before publishing. This paper has made use of the NASA/IPAC Extragalactic Database (NED) which is operated by the Jet Propulsion Laboratory, California Institute of Technology, under contract with the National Aeronautics and Space Administration. Funding for the Sloan Digital Sky Survey (SDSS) has been provided by the Alfred P. Sloan Foundation, the Participating Institutions, the National Aeronautics and Space Administration, the National Science Foundation, the U.S. Department of Energy, the Japanese Monbukagakusho, and the Max Planck Society. The SDSS Web site is http://www.sdss.org/. The SDSS is managed by the Astrophysical Research Consortium (ARC) for the Participating Institutions. The Participating Institutions are The University of Chicago, Fermilab, the Institute for Advanced Study, the Japan Participation Group, The Johns Hopkins University, the Korean Scientist Group, Los Alamos National Laboratory, the Max-Planck-Institute for Astronomy (MPIA), the Max-Planck-Institute for Astrophysics (MPA), New Mexico State University, University of Pittsburgh, University of Portsmouth, Princeton University, the United States Naval Observatory, and the University of Washington.

REFERENCES

Akujor C. E., Porcas R. W., Smoker J. V., 1996, A&A, 306, 391

Alexander P., 2000, MNRAS, 319, 8

Aller M. F., Aller H. D., Hughes P. A., 1992, ApJ, 399, 16

Allington-Smith J. R., Spinrad H., Djorgovski S., Liebert J., 1988, MNRAS, 234, 1091

Anton S., Thean A. H. C., Pedlar A., Browne I. W. A., 2002, MNRAS, 336, 319

Augusto P., Wilkinson P. N., 2001, MNRAS, 320, L40

Augusto P., Wilkinson P. N., Browne I. W. A., 1998, MNRAS, 299, 1159

Augusto P., Edge A. C., Chandler C. J., 2005, MNRAS, submitted

Augusto P., 1996, Ph.D. Thesis, University of Manchester, UK

Baldwin J. A., Burbidge E. M., Hazard C., Murdoch H. S., Robinson L. B., Wampler E. J., 1973, ApJ, 185, 739

Bartel N. et al., 1984, ApJ, 279, 116

Baum S. A., O'Dea C. P., de Bruyn A. G., Murphy D. W., 1990, A&A, 232, 19

Beasley A. J., Gordon D., Peck A. B., Petrov L., MacMillan D. S., Fomalont E. B., Ma C., 2002, ApJS, 141, 13

Begelman M. C., 1996, in Carilli C. L., Harris D. E., eds, Cygnus A — Study of a Radio Galaxy (Proc. of Greenbank workshop). Cambridge University Press, p. 209

Blandford R. D., Rees M. J., 1974, MNRAS, 169, 395

Bondi M., Garrett M. A., Gurvits L. I., 1998, MNRAS, 297, 559

Bondi M., Marcha M. J. M., Dallacasa D., Stanghellini C., 2001, MNRAS, 325, 1109

Burbidge G., Crowne A. H., 1979, ApJS, 40, 583

Carilli C. L., Menten K. M., Reid M. J., Rupen M. P., Yun M. S., 1998, ApJ, 494, 175

Carvalho J. C., 1985, MNRAS, 215, 463

Clements D. L., McDowell J. C., Shaked S., Baker A. C., Borne K., Colina L., Lamb S. A., Mundell C., 2002, ApJ, 581, 974

Cohen J. G., Lawrence C. R., Blandford R. D., 2003, ApJ, 583, 67

Condon J. J., Kaplan D. L., 1998, ApJS, 117, 361

Condon J. J., Cotton W. D., Greisen E. W., Yin Q. F., Perley R. A., Taylor G. B., Broderick J. J., 1998, AJ, 115, 1693

Condon J. J., Cotton W. D., Broderick J. J., 2002, AJ, 124, 675

Conway J. E., Pearson T. J., Readhead A. C. S., Unwin S. C., Xu W., Mutel R. L., 1992, ApJ, 396, 62

Conway J. E., Myers S. T., Pearson T. J., Readhead A. C. S., Unwin S. C., Xu W., 1994, ApJ, 425, 568

Cotton W. D., Feretti L., Giovannini G., Venturi T., Lara L., Marcaide J., Wehrle A. E., 1995, ApJ, 452, 605

Dallacasa D., Fanti C., Fanti R., Schilizzi R. T., Spencer R. E., 1995, A&A, 295, 27

Dallacasa D., Bondi M., Alef W., Mantovani F., 1998, A&AS, 129, 219

Dallacasa D., Tinti S., Fanti C., Fanti R., Gregorini L., Stanghellini C., Vigotti M., 2002a, A&A, 389, 115

Dallacasa D., Fanti C., Giacintucci S., Stanghellini C., Fanti R., Gregorini L., Vigotti M., 2002b, A&A, 389, 126

de Vaucouleurs G., de Vaucouleurs A., Corwin Jr. H. G., Buta R. J., Paturel G., Fouqué P., 1991, in "Third Reference Catalogue of Bright Galaxies". Springer-Verlag

de Vries W. H., Barthel P. D., Hes R., 1995, A&AS, 114, 259

de Vries W. H. et al., 1997, ApJS, 110, 191

de Vries W. H., O'Dea C. P., Perlman E., Baum S. A., Lehnert M. D., Stocke J., Rector T., Elston R., 1998a, ApJ, 503, 138

de Vries W. H., O'Dea C. P., Baum S. A., Perlman E., Lehnert M. D., Barthel P. D., 1998b, ApJ, 503, 156

de Vries W. H., O'Dea C. P., Barthel P. D., Fanti C., Fanti R., Lehnert M. D., 2000, AJ, 120, 2300

de Young D. S., 1997, ApJ, 490, L55

Dondi L., Ghisellini G., 1995, MNRAS, 273, 583

Drinkwater M. J. et al., 1997, MNRAS, 284, 85

Emerson J. P., Clegg P. E., Gee G., Griffin M. J., Cunningham C. T., Brown L. M. J., Robson E. I., Longmore A. J., 1984, Nature, 311, 237

Falco E. E., Kochanek C. S., Munoz J. A., 1998, ApJ, 494, 47

Fanaroff B. L., Riley J. M., 1974, MNRAS, 167, P31

Fanti R., Fanti C., Schilizzi R. T., Spencer R. E., Nan R., Parma P., van Breugel W. J. M., Venturi T., 1990, A&A, 231, 333

Fanti C., Fanti R., Dallacasa D., Schilizzi R. T., Spencer R. E., Stanghellini C., 1995, A&A, 302, 317

Fanti C., Pozzi F., Dallacasa D., Fanti R., Gregorini L., Stanghellini C., Vigotti M., 2001, A&A, 369, 380

Fassnacht C. D., Taylor G. B., 2001, AJ, 122, 1661

Fey A. L., Clegg A. W., Fomalont E. B., 1996, ApJS, 105, 299

Fomalont E. B., Frey S., Paragi Z., Gurvits L. I., Scott W. K., Taylor A. R., Edwards P. G., Hirabayashi H., 2000, ApJS, 131, 95

Gallimore J. F., Baum S. A., O'Dea C. P., Pedlar A., Brinks E., 1999, ApJ, 524, 684

Giovannini G., Cotton W. D., Feretti L., Lara L., Venturi T., 2001, ApJ, 552, 508

Giroletti M., Giovannini G., Taylor G. B., Conway J. E., Lara L., Venturi T., 2003, A&A, 399, 889

Giroletti M., Giovannini G., Taylor G. B., 2005, A&A, 441, 89

Goncalves A. C., Veron P., Veron-Cetty M.-P., 1998, A&AS, 127, 107

Gorshkov A. G., Konnikova V. K., Mingaliev M. G., 2003, Astron. Rep., 47, 903

Graham J. R., Carico D. P., Matthews K., Neugebauer G., Soifer B. T., Wilson T. D., 1990, ApJ, 354, L5

Gregory P. C., Condon J. J., 1991, ApJS, 75, 1011

Gregory P. C., Scott W. K., Douglas K., Condon J. J., 1996, ApJS, 103, 427

Gugliucci N. E., Taylor G. B., Peck A. B., Giroletti M., 2005, ApJ, 622, 136

Heckman T. M., Dahlem M., Eales S. A., Fabbiano G., Weaver K., 1996, ApJ, 457, 616

Henstock D. R., Browne I. W. A., Wilkinson P. N., Taylor G. B., Vermeulen R. C., Pearson T. J., Readhead A. C. S., 1995, ApJS, 100, 1

Henstock D. R., Browne I. W. A., Wilkinson P. N., McMahon R. G., 1997, MNRAS, 290, 380

Herbig T., Readhead A. C. S., 1992, ApJS, 81, 83

Hewett P. C., Foltz C. B., Chaffee F. H., 1995, AJ, 109, 1498

Hewitt A., Burbidge G., 1989, ApJS, 63, 1

Hewitt A., Burbidge G., 1991, ApJS, 75, 297

Hintzen P., Ulvestad J., Owen F., 1983, AJ, 88, 709

Hooimeyer J. R. A., Schilizzi R. T., Miley G. K., Barthel P. D., 1992, A&A, 261, 25

Hook I. M., McMahon R. G., 1998, MNRAS, 294, L7

Hook I. M., McMahon R. G., Irwin M. J., Hazard C., 1996, MNRAS, 282, 1274

Kaiser C. R., Alexander P., 1997, MNRAS, 286, 215

Kellerman K. I., Vermeulen R. C., Zensus J. A., Cohen M. H., 1998, AJ, 115, 1295

Kunert-Bajraszewska M., Marecki A., Thomasson P., Spencer R. E., 2005, A&A, 440, 93

Kunert M., Marecki A., Spencer R. E., Kus A. J., Niezgoda J., 2002, A&A, 391, 47

Lara L., Cotton W. D., Feretti L., Giovannini G., Marcaide J. M., Marquez I., Venturi T., 2001, A&A, 370, 409

Le Borgne J.-F., Mathez G., Mellier Y., Pelló R., Sanahuja B., Soucail G., 1991, A&AS, 88, 133

Lonsdale C. J., Barthel P. D., Miley G. K., 1998, ApJS, 87, 63

Magliocchetti M. et al., 2004, MNRAS, 350, 1485

Marcha M. J. M., Browne I. W. A., Impey C. D., Smith P. S., 1996, MNRAS, 281, 425

Marecki A., Falcke H., Niezgoda J., Garrington S. T., Patnaik A. R., 1999, A&AS, 135, 273

Marecki A., Spencer R. E., Kunert M., 2003, PASA, 20, 46

Middelberg E. et al., 2004, A&A, 417, 925

Miller N. A., Owen F. N., 2001, ApJS, 134, 355

Miller N. A., Ledlow M. J., Owen F. N., Hill J. M., 2002, AJ, 123, 3018

Munoz J. A., Falco E. E., Kochanek C. S., Lehar J., Mediavilla E., 2003, ApJ, 594, 684

Murgia M., Fanti C., Fanti R., Gregorini L., Klein U., Mack K.-H., Vigotti M., 1999, A&A, 345, 769

Norris R. P., Baan W. A., Haschick A. D., Diamond P. J., Booth R. S., 1985, MNRAS, 213, 823

Norris R. P., 1988, MNRAS, 230, 345

O'Dea C. P., Baum S. A., Stanghellini C., 1991, ApJ, 380, 66

O'Dea C., 1998, PASP, 110, 493

Ojha R., Fey A. L., Johnston K. J., Jauncey D. L., Tzioumis A. K., Reynolds J. E., 2004, AJ, 127, 1977

Orienti M., Dallacasa D., Fanti C., Fanti R., Tinti S., Stanghellini C., 2004, A&A, 426, 463

Owsianik I., Conway J. E., Polatidis A. G., 1998, A&A, 336, L37

Patnaik A. R., Browne I. W. A., Wilkinson P. N., Wrobel J. M., 1992a, MNRAS, 254, 655

Patnaik A. R., Browne I. W. A., Walsh D., Chaffee F. H., Foltz C. B., 1992b, MNRAS, 259, P1

Peacock J. A., Wall J. V., 1982, MNRAS, 198, 843

Peck A. B., Taylor G. B., 2000, ApJ, 534, 90

Peck A. B., Taylor G. B., Fassnacht C. D., Readhead A. C. S., Vermeulen R. C., 2000, ApJ, 534, 104

Perlman E. S., Stocke J. T., Shaffer D. B., Carilli C. L., Ma C., 1994, ApJ, 424, L69

Perlman E. S., Carilli C. L., Stocke J. T., Conway J., 1996, AJ, 111, 1839

Perlman E. S., Padovani P., Giommi P., Sambruna R., Jones L. R., Tzioumis A., Reynolds J., 1998, AJ, 115, 1253

Perlman E. S., Stocke J. T., Conway J., Reynolds C., 2001, AJ, 122, 536

Perucho M., Martí J. M., 2002, ApJ, 568, 639

Phillips R. B., Mutel R. L., 1982, A&A, 106, 21

Polatidis A. G., Conway J. E., 2003, PASA, 20, 69

Polatidis A. G., Wilkinson P. N., Xu W., Readhead A. C. S., Pearson T. J., Taylor G. B., Vermeulen R. C., 1995, ApJS, 98, 1

Polatidis A. G., Wilkinson P. N., Xu W., Readhead A. C. S., Pearson T. J., Taylor G. B., Vermeulen R. C., 1999, New Astron. Rev., 43, 657

Puchnarewicz E. M., Mason K. O., Cordova F. A., Kartje J., Brabduardi-Raymont G., Mittaz J. P. D., Murdin P. G., Allington-Smith J., 1992, MNRAS, 256, 589

Readhead A. C. S., Taylor G. B., Xu W., Pearson T. J., Wilkinson P. N., 1996a, ApJ, 460, 612

Readhead A. C. S., Taylor G. B., Pearson T. J., Wilkinson P. N., 1996b, ApJ, 460, 634

Reid A., Shone D. L., Akujor C. E., Browne I. W. A., Murphy D. W., Pedelty J., Rudnick L., Walsh D., 1995, A&AS, 110, 213

Rossetti A., Mantovani F., Dallacasa D., Fanti C., Fanti R., 2005, A&A, 434, 449

Rovilos E., Diamond P. J., Lonsdale C. J., Smith H. E., 2003, MNRAS, 342, 373

Saikia D. J., Junor W., Cornwell T. J., Muxlow T. W. B., Shastri P., 1990, MNRAS, 245, 408

Saikia D. J., Jeyakumar S., Mantovani F., Salter C. J., Spencer R. E., Thomasson P., Wiita P. J., 2003, PASA, 20, 50

Sanghera H. S., Saikia D. J., Luedke E., Spencer R. E., Foulsham P. A., Akujor C. E., Tzioumis A. K., 1995, A&A, 295, 629

Sargent W. L. W., 1973, ApJ, 182, L13

Scoville N. Z. et al., 1998, ApJ, 492, L107

Shaya E. J., Dowling D. M., Currie D. G., Faber S. M., Groth E. J., 1994, AJ, 107, 1675

Snellen I. A. G., Schilizzi R. T., Bremer M. N., Miley G. K., de Bruyn A. G., Rottgering H. J., 1999, MNRAS, 307, 149

Snellen I. A. G., Schilizzi R. T., van Langevelde H. J., 2000, MNRAS, 319, 429

Soifer B. T. et al., 1984, ApJ, 283, L1

Sowards-Emmerd D., Romani R. W., Michelson P. F., 2003, ApJ, 590, 109

Spencer R. E., McDowell J. C., Charlesworth M., Fanti C., Parma P., Peacock J. A., 1989, MNRAS, 240, 657

Stanghellini C., O'Dea C. P., Baum S. A., Dallacasa D., Fanti R., Fanti C., 1997a, A&A, 325, 943

Stanghellini C., Bondi M., Dallacasa D., O'Dea C. P., Baum S. A., Fanti R., Fanti C., 1997b, A&A, 318, 376

Stanghellini C., O'Dea C. P., Dallacasa D., Baum S. A., Fanti R., Fanti C., 1998, A&AS, 131, 303

Stanghellini C., O'Dea C. P., Murphy D. W., 1999, A&AS, 134, 309

Stanghellini C., Dallacasa D., O'Dea C. P., Baum S. A., Fanti R., Fanti C., 2001, A&A, 377, 377

Stickel M., Kuhr H., 1993, A&AS, 101, 521

Stickel M., Kuhr H., 1996, A&AS, 115, 1

Stickel M., Rieke G. H., Kuhr H., Rieke M. J., 1996, ApJ, 468, 556

Sykes C. M., 1997, Ph.D. Thesis, University of Manchester, UK

Tadhunter C. N., Morganti R., di Serego-Alighieri S., Fosbury R. A. E., Danziger I. J., 1993, MNRAS, 263, 999

Taylor G. B., Peck A. B., 2003, ApJ, 597, 157

Taylor G. B., Vermeulen R. C., 1997, ApJ, 485, L9

Taylor G. B., Vermeulen R. C., Pearson T. J., Readhead A. C. S., Henstock D. R., Browne I. W. A., Wilkinson P. N., 1994, ApJS, 95, 345

Taylor G. B., Readhead A. C. S., Pearson T. J., 1996a, ApJ, 463, 95

Taylor G. B., Vermeulen R. C., Readhead A. C. S., Pearson T. J., Henstock D. R., Wilkinson P. N., 1996b, ApJS, 107, 37

Taylor G. B., Vermeulen R. C., Readhead A. C. S., Pearson T. J., Henstock D. R., Wilkinson P., 1997, in Snellen I. A. G., Schilizzi R. T., Rottgering H. J. A., Bremer M. N., eds, The Second Workshop on Gigahertz Peaked Spectrum and Compact Steep Spectrum Radio Sources. Leiden Observatory

Taylor G. B., Wrobel J. M., Vermeulen R. C., 1998, ApJ, 498, 619

Taylor G. B., Marr J. M., Pearson T. J., Readhead A. C. S., 2000, ApJ, 541, 112

Taylor G. B. et al., 2005, ApJS, 159, 27

Thompson D., Djorgovski S., de Carvalho R., 1990, PASP, 102, 1235

Torniainen I., Tornikoski M., Terasranta H., Aller M. F., Aller H. D., 2005, A&A, 435, 839

Tornikoski M., Jussila I., Johansson P., Lainela M., Valtaoja E., 2001, AJ, 121, 1306

Tschager W., Schilizzi R. T., Rottgering H. J. A., Snellen I. A. G., Miley G. K., 2000, A&A, 360, 887

Tschager W., Schilizzi R. T., Rottgering H. J. A., Snellen I. A. G., Miley G. K., Perley R. A., 2003, A&A, 402, 171

Tzioumis A. et al., 1989, AJ, 98, 36

Tzioumis A. K. et al., 2002, A&A, 392, 841

Unger S. W., Pedlar A., Neff S. G., de Bruyn A. G., 1984, MNRAS, 209, 15P

Unger S. W., Pedlar A., Booler R. V., Harrison B. A., 1986, MNRAS, 219, 387

Vermeulen R. C., Taylor G. B., 1995, AJ, 109, 1983

Vermeulen R. C., Taylor G. B., Redhead A. C. S., Browne I. W. A., 1996, AJ, 111, 1013

Wegner G., Colless M., Saglia R. P., McMahan R. K., Davies R. L., Burstein D., Baggley G., 1999, MNRAS, 305, 259

White R. L., Becker R. H., 1992, ApJS, 79, 331

White R. L., Kinney A. L., Becker R. H., 1993, ApJ, 407, 456

Wiklind T., Combes F., 1997, A&A, 328, 48

Wilkinson P. N., Polatidis A., Readhead A. C. S., Xu W., Person T. J., 1994, ApJ, 432, L87

Wilkinson P. N., 1995, Proc. Natl. Acad. Sci, 92, 11342

Willott C. J., Rawlings A., Blundell K. M., Lacy M., 1998, MNRAS, 300, 625

Wills D., Wills B. J., 1976, ApJS, 31, 143

Xu W., Lawrence C. R., Readhead A. C. S., Pearson T. J., 1994, AJ, 108, 395

Xu W., Readhead A. C. S., Pearson T. J., Polatidis A. G., Wilkinson P. N., 1995, ApJS, 99, 297

Yee H. K. C., Ellingson E., Abraham R. G., Gravel P.,

Carlberg R. G., Smecker-Hane T. A., Schade D., Rigler M., 1996, ApJS, 102, 289

Zensus J. A., Ros E., Kellermann K. I., Cohen M. H., Vermeulen R. C., Kadler M., 2002, AJ, 124, 662

APPENDIX A: COMMENTS ON PREVIOUS RELATED PAPERS

In what follows, in two separate sections, we discuss the implications of the new parent sample (1743 sources vs. the old 1665) and main sample (157 sources vs. the old 55) sizes and membership to the two main related papers, Augusto et al. (1998) and Augusto & Wilkinson (2001).

A1 Augusto et al. (1998)

Well after publishing this paper, we found that one of the 55-sample sources (B1947+677) had a significantly wrong position. It should have read (J2000.0): 19:47:36.2599 (RA) and 67:50:16.928 (dec). This has been corrected in Tables 4 and 5. In addition, there are now new $\alpha_{1.40}^{4.85}$ values for seven of the Augusto et al. (1998) Table 2 (Column (7)) 55-sample sources while five others (B0352+825, B0819+082, B0905+420, B1801+036, B2101+664) should be left with blanks (rather than fill them with spectral indices from sources other than White & Becker (1992) and Gregory & Condon (1991)): −0.02 (B0218+357); 0.25 (B0821+394); 0.24 (B0831+557); 0.22 (B0916+718); 0.47 (B1143+446); 0.38 (B1947+677); 0.04 (B2201+044).

As regards the statistical conclusions of Augusto et al. (1998) we must revise them by comparing the "old" and the "new" situations, now that we have both revised the parent sample and the 55-source sample (which, now, has all its sources included in the larger 157-source sample). We focus on the $\alpha_{1.40}^{4.85}$ distribution only. Starting with the parent samples we first note that, while for the new sample we used the maximum number possible of values (1311) for the old one a representative sub-sample of 373 sources was selected and it is from this one that the statistics of Augusto et al. (1998) are worked out. Comparing both through a KS-test we cannot reject the hypothesis that they are similar. Finally, comparing the $\alpha_{1.40}^{4.85}$ distributions for the 157-source (actually 123 values) and 55-source samples through a KS-test we cannot reject the hypothesis that they are similar.

A2 Augusto & Wilkinson (2001)

The only result from Augusto & Wilkinson (2001) that is affected by the change from the old 1665-source parent sample to the new 1743-source one relates to their different sizes: the quoted maximum multiple imaging lensing rate on $10^{9.5}$–$10^{10.9} M_{\odot}$ (160–300 mas angular separation of images) of 1:555 (95% confidence level) actually improves to 1:581 at the same confidence level. As regards to the main result of the paper (limits on the density of compact objects within the above mass range of $\Omega_{CO} < 0.1$ at 95% confidence), this remains unchanged since the 5% increase in sample size does not cause significant effects.

Table 2. The collection of confirmed CSOs from the literature (selected among all sources that have ever been called CSO, MSO, GPS, CSS or CD
(1): Source name; *there are comments in the text; **(2), (3):** source position from the NASA Extragalactic Database (NED); **(4):** the optical host type
Q — QSO; **(5), (6):** the source redshift ('p' indicates a photometric estimate) and reference (listed at the end of this caption); **(7):** classification —
in column (17); 'CSO?' indicates that this source still might be an MSO, depending on its linear size; **(8):** references with the relevant maps that all
the end of this caption); **(9):** the interferometer(s) used that allow final classification: V (VLA), M (MERLIN) or VL (VLBI); the interferometer that p
in the determinations of Columns (13)–(16) is indicated in bold; **(10):** the measured largest angular size between either 6σ or 5σ (marked *) contou
frequencies — are indicated as superscripts); **(11):** spectral index $\alpha_{1.40}^{4.85}$ with flux densities (at 1.40 GHz and 4.85 GHz) from White & Becker (1992)
respectively; **(12):** when possible (> 2 points), the fitted spectral index to the thin part of the overall spectrum (as in NED); A — peakless, complex spec
is the estimated spectrum peak (in GHz) while as subscripts we use: s — steepening spectrum from peak; v — variable source; 3 — only three points us
(5 GHz); exceptions (other frequencies) are indicated as superscripts; **(14):** $S^{peak}_{bright-lobe}/S^{peak}_{faint-lobe}$ (5 GHz); exceptions (other frequencies) are indica
length ratio (5 GHz); exceptions (other frequencies) are indicated as superscripts; **(16):** the 'arm angle' (5 GHz), measured between the opposed lobes
are indicated as superscripts; **(17):** the projected linear size in kpc (from Columns (5) and (10)); **(18):** the $\log_{10}$ 1.4 GHz power in W/Hz (data fro
references for Columns (6) and (8): 1– Phillips & Mutel (1982); 2– Herbig & Readhead (1992); 3– Dallacasa et al. (1995); 4– Fey et al. (1996); 5– Keller
al. (2002); 7– The NASA Extragalactic Database (NED); 8– Gallimore et al. (1999); 9– Stanghellini et al. (2001); 10– Stanghellini et al. (1997b); 11– Cot
al. (2002); 13– Fomalont et al. (2000); 14– Taylor et al. (1994); 15– Dallacasa et al. (2002a); 16– Dallacasa et al. (2002b); 17– Carilli et al. (1998); 18– Ov
et al. (2000); 20– Peck & Taylor (2000); 21– Giovannini et al. (2001); 22– Marcha et al. (1996); 23– Sanghera et al. (1995); 24– Hewitt & Burbidge (1991
Australia Telescope National Facility, Wright & Otrupcek, (Eds); 26– Xu et al. (1995); 27– Polatidis et al. (1995); 28– Taylor et al. (1996a); 29– Taylo
al. (2000a); 31– Stanghellini et al. (1997a); 32– Stickel & Kuhr (1993); 33– Stanghellini et al. (1999); 34– Akujor et al. (1996); 35– Conway et al. (1992
37– Aller et al. (1992); 38— de Vries et al. (1995); 39– Bondi et al. (1998); 40– Augusto et al. (1998); 41– Unger et al. (1984); 42– Unger et al. (1986); 4
Wiklind & Combes (1997); 45– Perlman et al. (1994); 46– Baum et al. (1990); 47– Perlman et al. (1996); 48– de Vries et al. (2000); 49– Snellen et al. (199
51– Tzioumis et al. (2002); 52– Ojha et al. (2004); 53– Tschager et al. (2000); 54– Bartel et al. (1984); 55– Conway et al. (1994); 56– Taylor & Vermeule
Wilkinson (1995); 59– Orienti et al. (2004); 60– Gugliucci et al. (2005); 61– Peck et al. (2000); 62– Miller et al. (2002); 63– Giroletti, Giovannini, and Ta

(1) Name	(2) RA (J2000.0)	(3) Dec (J2000.0)	(4) Id.	(5) z	(6) Ref.	(7) Class.	(8) Ref.	(9) Tel.	(10) LAS ($''$)	(11) $\alpha_{1.40}^{4.85}$	(12) α_{thin}	(13) S_n/S_{bl}	(14) S_{bl}/S_{fl}	
4C+40.52	00h00m53.0815s	+40°54'01.793"	G			CSO	6,15,20,59	VL	0.10	0.51	$0.6^{0.4}_{s}$	0.19	28	
B0001+478	00h03m46.0412s	+48°07'04.133"				CSO	20	VL	0.015	0.60	0.6_{3}	0.08	1.5	
B0026+346	00h29m14.2424s	+34°56'32.247"	G	0.517	12	CSO	5,6,13,14	VL	0.040	0.23	0.3^{1}	0.040	3.3	
B0046+316*	00h48m47.1438s	+31°57'25.094"	G	0.015	42	CSO	40,41	M	0.38	0.05	0_{v}	5.0	2.7	
B0108+388	01h11m37.3169s	+39°06'28.104"	G	0.668	17	CSO	12,18,19,46	VL	0.008^{15}	−0.94	1.0^{5}_{s}	0.08^{15}	1.4^{15}	1
4C+31.04	01h19m34.9991s	+32°10'50.013"	G	0.060	22	CSO	11,21,40	VL	0.11	0.47	$0.4^{0.4}$	0.7	3.5	
B0147+400	01h50m19.623s	+40°17'29.98"				CSO	15,59	VL	0.075	0.67	0.6_{s}	0.17	12	
B0201+088	02h04m34.7591s	+09°03'49.259"				CSO	6,20	VL	0.037	0.75	—[1]	1.5	1.1	
B0222+36	02h25m27.351s	+37°10'27.56"	G	0.033	62	CSO	63	**V**+VL	$1.2^{8.4}$	0.53	0.4_{3}	$6.6^{8.4}$	$3.1^{8.4}$	1
B0233+434	02h37m01.2149s	+43°42'04.191"				CSO	40	M+**VL**	0.14	0.45	$0.5^{0.4}_{3}$	< 0.006	2.2	
B0352+825	04h02m12.6736s	+82°41'35.103"				CSO	40	M+**VL**	0.069	—	—	5.4	3.6	
B0423−163	04h25m53.5726s	−16°12'40.248"				CSO	29	VL	0.096	—	0.6_{s}	0.035	7.1	
B0424+414*	04h27m46.0455s	+41°33'01.099"				CSO	20	VL	0.006^{15}	−0.10	—[5]	39^{15}	1.4^{15}	1
B0428+205	04h31m03.7585s	+20°37'34.189"	G	0.219	25	CSO	3,58	**M**+VL	$0.32^{1.7}$ *	0.20	0.6^{1}_{s}	$0.06^{1.7}$	$31^{1.7}$	4
B0500+019*	05h03m21.1971s	+02°03'04.677"	G	0.585	17	CSO	9,31	VL	0.017	0.09	0.5^{3}	1.7	2.2	
B0646+600*	06h50m31.2543s	+60°01'44.555"	Q	0.455	32	CSO	26,33,34	VL	0.009	−0.59	0.5^{4}_{s}	0.83	113	
B0703+468*	07h06m48.037s	+46°47'56.22"	Q?			CSO	15,23,59	V+**VL**	0.065	0.67	$0.5^{0.4}_{3,s}$	< 0.005	1.6	
B0710+439*	07h13m38.1641s	+43°49'17.205"	G	0.518	35	CSO	19,28,35,36	VL	0.026	0.09	0.4^{2}	0.68	4.3	
4C+39.17	07h25m49.993s	+39°17'25.47"	G			CSO?	16	V+**VL**	$0.42^{1.7}$	1.26	$1.1^{0.4}_{3,s}$	$< 0.02^{1.7}$	$20^{1.7}$	
B0750+535	07h54m15.2176s	+53°24'56.449"				CSO	20	VL	0.026	0.59	$0.8^{1}_{3,s}$	0.18	1.0	
B0840+424A	08h43m31.6374s	+42°15'29.525"				CSO	15,59	VL	0.12	0.64	$0.6^{0.4}_{s}$	< 0.2	19	
B1031+567	10h35m07.0403s	+56°28'46.798"	G	0.45	37	CSO	13,19,30	VL	0.038	0.31	$0.5^{0.8}$	< 0.004	3.1	
J1111+1955	11h11m20.0658s	+19°55'36.001"	G	0.299	67	CSO	20	VL	$0.020^{8.4}$	0.46	0.5^{1}_{3}	$< 0.02^{8.4}$	$2.0^{8.4}$	
4C+14.41	11h20m27.8043s	+14°20'55.020"	G	0.362	38	CSO	6,23,39	**M**+VL	0.11^{23}	0.82	$0.5^{0.4}_{s}$	1.1^{23}	2.9^{23}	1
B1208−192	12h11m31.801s	−19°34′19.95"	Q	2.054	24	CSO	31	VL	0.023^{15}	—	0.6	0.042^{15}	1.9^{15}	1
4C+32.44	13h26m16.5124s	+31°54'09.514"	G	0.370	2	CSO	1,3,4,5	VL	$0.071^{8.6}$	0.61	$0.6^{0.4}$	$< 0.02^{8.6}$	$2.0^{8.6}$	
4C+62.22	14h00m28.593s	+62°10'40.11"	G	0.431	7	CSO	3,28	VL	$0.060^{8.4}$	0.70	$0.7^{0.6}$	$1.0^{8.4}$	$1.1^{8.4}$	2
Mrk 668	14h07m00.3944s	+28°27'14.690"	G	0.077	8	CSO	5,9,10	VL	0.009^{15}	−0.93	1.1^{6}_{v}	0.013^{15}	61^{15}	1

(1) Name	(2) RA (J2000.0)	(3) Dec (J2000.0)	(4) Id.	(5) z	(6) Ref.	(7) Class.	(8) Ref.	(9) Tel.	(10) LAS ($''$)	(11) $\alpha_{1.40}^{4.85}$	(12) α_{thin}	(13) S_n/S_{bl}	(14) S_{bl}/S_{fl}	(
B1413+135	14h15m58.8174s	+13°20'23.713"	Q	0.247	44	CSO	5,13,20,45,47	VL	$0.18^{1.7}$	0.29	A	$1.6^{1.7}$	$22^{1.7}$	2
B1543+005	15h46m09.5314s	+00°26'24.613"	G	0.556	48	CSO	6,13,20,60	VL	0.017	0.26	0.4	10	1.3	
B1732+094	17h34m58.3769s	+09°26'58.259"	G	0.61^{p}	33	CSO	6,20,33	VL	0.017	0.01	0.1_3	< 0.01	2.0	
B1801+036	18h03m56.2829s	+03°41'07.575"	G			CSO?	40	M	1.35	—	—	3.8	8.0	
B1819+671	18h19m44.391s	+67°08'47.18"	G	0.220	49	CSO	30	VL	0.025	0.83	$—^{0.6}$	0.091	2.0	
B1824+185	18h26m17.7108s	+18°31'52.889"				CSO	6,20,60	VL	0.069	0.52	0.4_3	0.043	14	
B1843+356	18h45m35.1088s	+35°41'16.726"	G	0.764	43	CSO	6,27,28	VL	$0.034^{1.6}$	0.21	$0.4_{3,s}$	$0.069^{1.6}$	$64^{1.6}$	1
B1928+681	19h28m20.5502s	+68°14'59.247"				CSO?	40	M+**VL**	0.17	0.41	$0.5^{0.3}$	6.8	2.0	
B1934−638*	19h39m25.0261s	−63°42'45.625"	G	0.183	50	CSO	51,52	VL	0.075	—	0.9^{1}_{s}	< 0.008	1.4	
B1946+708	19h45m53.5199s	+70°55'48.732"	G	0.101	49	CSO	30,56	VL	0.038	0.29	0.4^{1}_{3}	0.25	14	
J1947+678	19h47m36.2599s	+67°50'16.928"				CSO?	40,57	**M**+VL	0.52	0.38	0.5_3	1.1	18	
B2021+614	20h22m06.6817s	+61°36'58.804"	G	0.227	24	CSO	27,53,54,55	VL	0.012	−0.20	0.4^{6}_{v}	0.83	9.7	
B2352+495	23h55m09.4586s	+49°50'08.341"	G	0.237	35	CSO	13,19,28,36	VL	0.055	0.33	0.6^{1}_{s}	9.1	1.4	